Technical Report Documentation Page

1. Report No. FHWA/TX-13/5-6048-01-1	2. Government Accession No.	3. Recipient's Catalog No.
4. Title and Subtitle Implementation of Centrifuge Testing for Swelling Properties of Highly Plastic Clays		5. Report Date March 2013; Published August 2013 6. Performing Organization Code
7. Author(s) Jorge G. Zornberg, Michael D. Plaisted, Christian P. Armstrong, and Trevor Walker		8. Performing Organization Report No. 5-6048-01-1
9. Performing Organization Name and Address Center for Transportation Research The University of Texas at Austin 1616 Guadalupe St., Suite 4.202 Austin, TX 78701		10. Work Unit No. (TRAIS) 11. Contract or Grant No. 5-6048-01
12. Sponsoring Agency Name and Address Texas Department of Transportation Research and Technology Implementation Office P.O. Box 5080 Austin, TX 78763-5080		13. Type of Report and Period Covered Technical Report 09/2007–08/2008 14. Sponsoring Agency Code

15. Supplementary Notes
Project performed in cooperation with the Texas Department of Transportation and the Federal Highway Administration.

16. Abstract

A novel centrifuge-testing device was developed for characterization of expansive soils, which are the source of major pavement design and maintenance problems across the state. Specifically, testing protocols were developed for use of a small centrifuge device to provide ***direct measurement*** of the vertical swelling of clays. In this test, soil samples are subjected to water infiltration during a comparatively short testing period. The centrifuge approach is well suited for pavement design because it provides not only one data point for a ***single*** normal stress but the ***entire*** relationship between vertical strains and vertical stresses. This feature represents a significant advantage over conventional swelling tests, which are prohibitively long; in addition, each conventional test provides the vertical strain for one vertical stress. Consequently, this approach is particularly well suited for use with the Potential Vertical Raise (PVR) approach.

The objective of this project is to quantify the benefits and implement the new centrifuge technology for characterization of expansive clays in Texas. This research team will achieve this objective by implementing the laboratory procedure developed as part of Research Project 0-6048 using multiple clay sources, developing a spreadsheet with swelling curves (vertical strain versus normal stress) for relevant high-plasticity clays in Texas, incorporating the use of swelling curves obtained using centrifuge technology into the PVR methodology, and developing training material that includes examples of practical problems for calculation of the PVR using actual swelling curves and actual subgrade profiles.

17. Key Words Highly plastic clay, swelling, and centrifugation	18. Distribution Statement No restrictions. This document is available to the public through the National Technical Information Service, Springfield, Virginia 22161; www.ntis.gov.

19. Security Classif. (of report) Unclassified	20. Security Classif. (of this page) Unclassified	21. No. of pages 90	22. Price

Form DOT F 1700.7 (8-72) Reproduction of completed page authorized

Implementation of Centrifuge Testing for Swelling Properties of Highly Plastic Clays

Jorge G. Zornberg, Ph.D., P.E.
Michael D. Plaisted
Christian P. Armstrong
Trevor M. Walker

CTR Technical Report:	5-6048-01-1
Report Date:	March 2013; Revised June 2013
Project:	5-6048-01
Project Title:	Pilot Implementation to Benefit from Centrifuge Technology for Characterization of Expansive Clays in the Austin District
Sponsoring Agency:	Texas Department of Transportation
Performing Agency:	Center for Transportation Research at The University of Texas at Austin

Project performed in cooperation with the Texas Department of Transportation and the Federal Highway Administration.

Center for Transportation Research
The University of Texas at Austin
1616 Guadalupe St., Suite 4.202
Austin, TX 78701
www.utexas.edu/research/ctr

Disclaimers

Author's Disclaimer: The contents of this report reflect the views of the authors, who are responsible for the facts and the accuracy of the data presented herein. The contents do not necessarily reflect the official view or policies of the Federal Highway Administration or the Texas Department of Transportation (TxDOT). This report does not constitute a standard, specification, or regulation.

Patent Disclaimer: There was no invention or discovery conceived or first actually reduced to practice in the course of or under this contract, including any art, method, process, machine manufacture, design or composition of matter, or any new useful improvement thereof, or any variety of plant, which is or may be patentable under the patent laws of the United States of America or any foreign country.

Engineering Disclaimer

NOT INTENDED FOR CONSTRUCTION, BIDDING, OR PERMIT PURPOSES.

Project Engineer: Jorge G. Zornberg
Professional Engineer License State and Number: CA No. C 056325
P. E. Designation: Research Supervisor

Acknowledgments

The authors express appreciation for the dedicated guidance of the TxDOT Project Director, Mr. Miguel Arellano. His input has been invaluable.

Products

Appendix A presents 5-6048-01-P2, *Swelling of Highly Plastic Clays under Centrifuge Loading*.

Table of Contents

List of Figures

List of Tables

Chapter 1. Introduction

The need to design and construct roadways on highly plastic clays is common in central and eastern Texas, where expansive clays are prevalent. Roadways constructed on highly plastic clay subgrades may be damaged as the result of significant volume changes that occur when these soils undergo cycles of wetting and drying. These volume changes induce vertical movements, accelerate the degradation of pavement materials, and ultimately shorten the service life of the roadway. Proper characterization of expansive clays is required for design of and remediation of roadways constructed on poor subgrade materials. Current methods for characterization of expansive clays, however, do not properly replicate field conditions, require excessive time for testing, or require the measurement of index properties rather than the direct measurement of swelling. An alternative method is implemented in this study, involving the infiltration of water into highly plastic clays under an increased gravity field in a centrifuge. This report consists of an examination of the changes in the procedures and equipment from the start of Project No. 5-6048-01 as well as the results from centrifuge testing, and a proposed new Potential Vertical Rise (PVR) approach incorporating results from the centrifuge testing.

In order to implement this method, the research group made use of a small centrifuge permeameter. In the testing setup, shown in Figure 1.1, water is ponded above the soil specimen and then the permeameter is spun around a central axis in order to create a high G-level environment that accelerates the flow of water into the highly plastic clay. The small centrifuge has an in-flight data acquisition system.

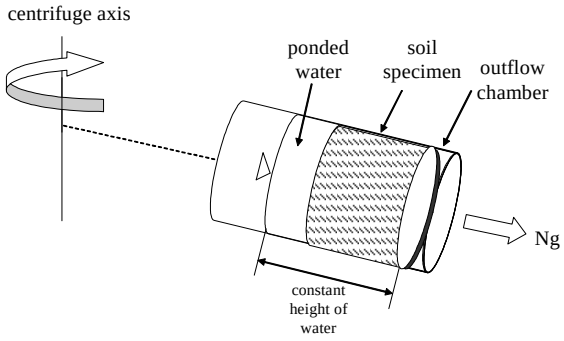

Figure 1.1: Centrifuge Testing Setup

Chapter 2. Soil Characterization

For the centrifuge testing project, five soils have been tested: the Eagle Ford shale, Houston Black clay, Black Taylor clay, Tan Taylor clay, and Soil 5, a backfill soil that was tested to compare the amount of swelling for a low plasticity soil. The first four soils consist of highly plastic clays that are known to be very expansive and costly in terms of road design and maintenance. Basic soil characterization tests were run, i.e., Atterberg limit tests (ASTM D 4318), sieve analysis (ASTM D 6913), organic matter tests (i.e., spectrometer tests), specific gravity tests (ASTM D 854-02), and standard proctor compaction tests (ASTM D 698). The research team also ran 1-g, or free swell, tests (ASTM D 4546) to compare those results with the centrifuge test results for three soils: the Eagle Ford shale, Houston Black clay, and Black Taylor clay.

2.1 Location and Preparation of Soil Samples

The soils were taken from the Austin District of the Texas Department of Transportation (TxDOT) at various points of construction or excavations. The Eagle Ford clay was taken from the intersection of Hester's Crossing and IH 35 in Round Rock using a backhoe at a depth of 3 meters (3.3 yards). The Houston Black clay was taken from the initial stages of a project on Highway 79 in Hutto from an excess stockpile of soil. The Black Taylor clay was taken from an excavation research project in Manor from excess stockpiled soil. The Tan Taylor clay was taken from a TxDOT project at the intersection of Highway 71 and Riverside in southeast Austin. The fifth soil was a backfill material taken from a TxDOT project site in the Austin District. Unfortunately, the precise location was not recorded when the sample was taken.

After being collected, the soils were processed by being air-dried, crushed with a sledge hammer, and then crushed into pieces via a soil crusher machine located at the University of Texas. Pebbles, roots, rocks, and other components that were larger than the number 10 sieve openings were removed prior to any testing to ensure the clay was isolated from other portions of the sublayer. Figure 2.1 has a map of the soil sample locations.

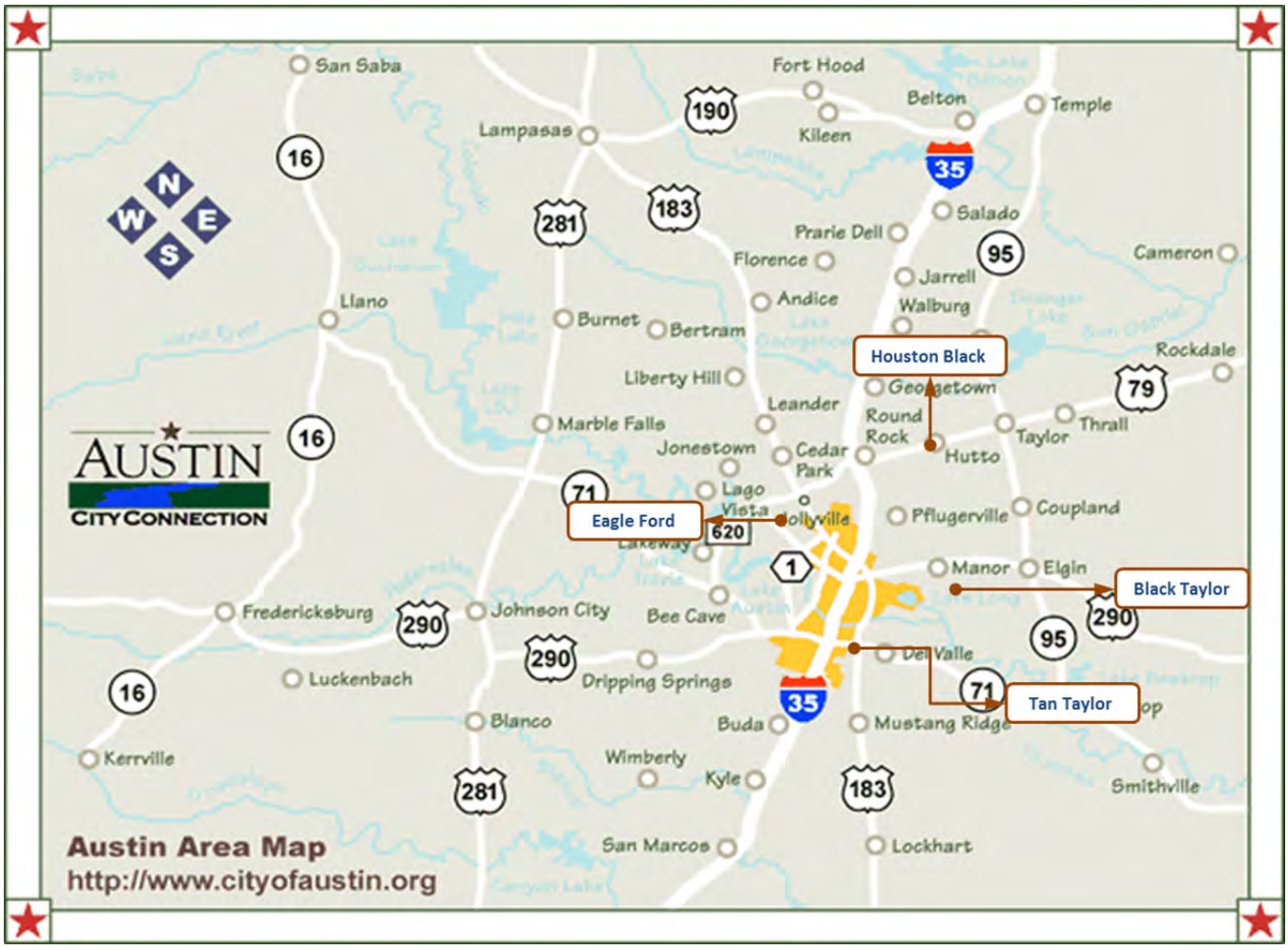

Figure 2.1: Location of Soil Samples for Centrifuge Testing

2.2 Conventional Characterization of Soils

After soil samples were prepared for each different soil, basic characterization tests were run. The index properties for these soils were measured in the Graduate Geotechnical lab at the University of Texas. The organic contents of the soil were tested at the TxDOT office using a spectrometer method. Figure 2.2 summarizes these properties for each soil.

Soil Property / Soil Type	Liquid Limit (LL)	Plastic Limit (PL)	Plasticity Index (PI)	Soil Classification (USCS)	Clay Content (%)	Organic Content (%)	Specific Gravity (Gs)	OMC (Std. Proctor) (%)	Max. Yd (Std. Proctor) (kN/m³)
Eagle Ford Clay	88	39	49	CH	64	0.07632	2.74	24.3	15.25
Houston Black Clay	62	27	35	CH	58	3.6741	2.701	25.5	14.72
Black Taylor Clay	55	28	27	CH	52	3.6747	2.712	23.3	15.34
Tan Taylor Clay	69	21	48	CH	-	-	2.76	22.5	15.68
Soil 5	25	14	11	CL	49	-	2.71	12.6	18.92

Figure 2.2: Soil Index Properties

Note that the Plasticity Index (PI) of Soil 5 is quite low, leading to an expectation that the soil does not expand upon wetting. The other four clays are classified as high PI clays, indicating that they have great potential for swelling upon wetting. The organic portion of the soil is not highly significant for testing purposes, and the specific gravity for all tests lies very near 2.70.

For the centrifuge testing project, the moisture content and dry density levels to compact at was determined via the standard proctor curves. Figure 2.3 compiles the standard proctor curve results. Note that Soil 5 has a much higher maximum dry unit weight and lower optimum moisture content as compared to the other four, high-PI soils.

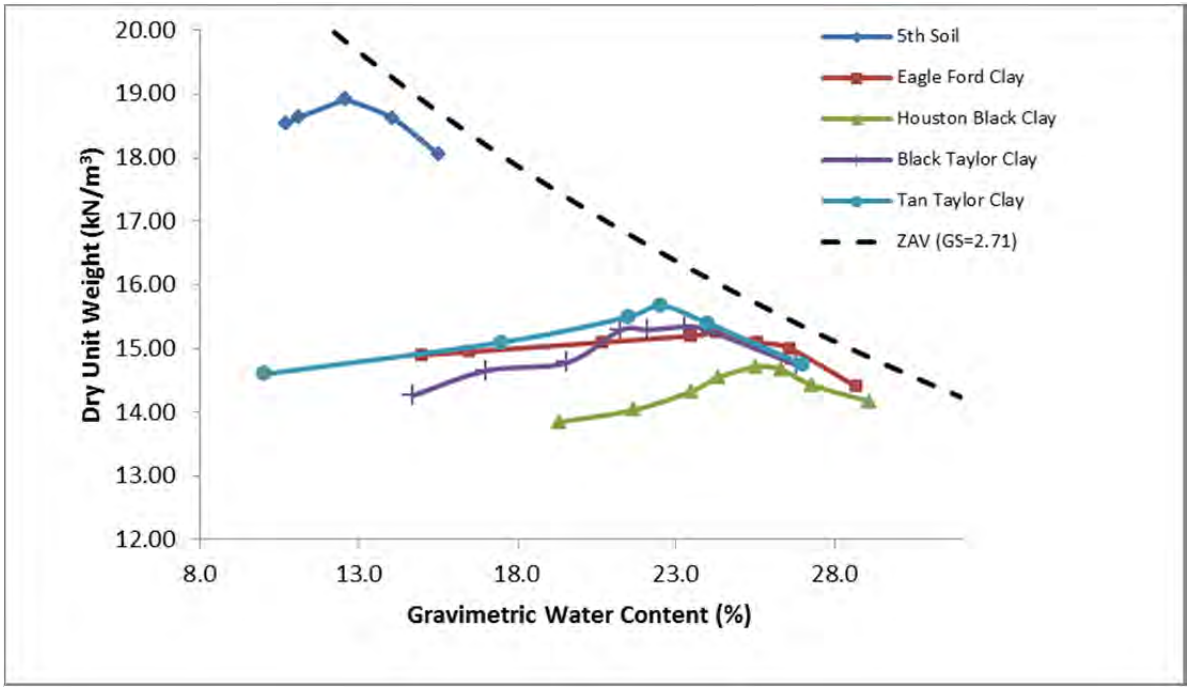

Figure 2.3: Standard Proctor Test Results for Soils

2.3 Standard Swell Tests Results

Standard swell testing was conducted according to ASTM D4546 Method A. The apparatus used for standard swell testing is the oedometer pictured in Figure 2.4. The soil specimen is placed in a fixed-ring consolidation cell, and the specimen is subjected to a confining pressure. During testing, vertical movements of the specimen were monitored with a dial gauge and a linear variable differential transducer (LVDT). After the specimen is placed in the apparatus and the seating load is applied, the height of the specimen is monitored. Once the height of the specimen comes to equilibrium, data is logged from the LVDT and water is added to the reservoir in which the soil specimen is sitting in order to begin swell testing. After 3 to 5 days, the sample would reach the equilibrium height; from this equilibrium height, the maximum swelling of the clay was recorded (as a percentage).

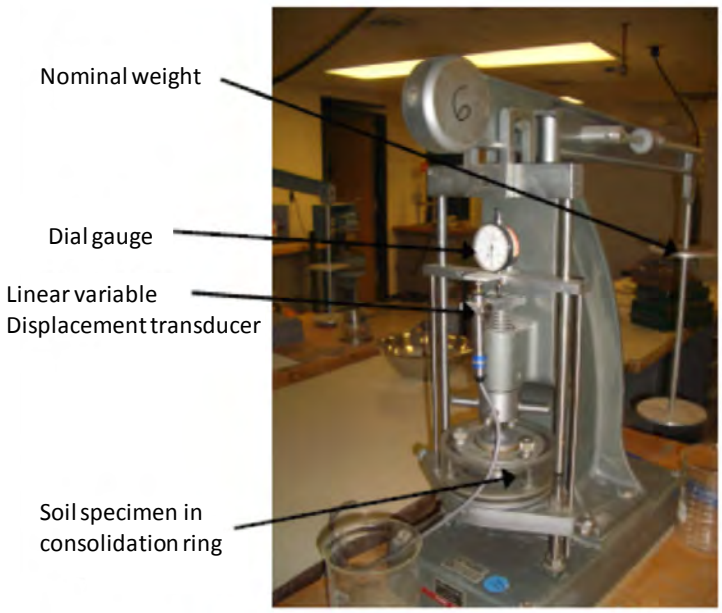

Figure 2.4: Oedometer Apparatus Used in Free-Swell Testing

The three soils selected for standard swell testing were the Eagle Ford, Houston Black, and Black Taylor clays. The Eagle Ford clay was subjected to the widest range of stresses, from 125 psf to 64,000 psf. The Houston Black and Black Taylor clays were subjected to stresses ranging from 125 psf to 2125 psf. The Eagle Ford clay was found to be the most expansive, swelling nearly 20% at a load of 125 psf. The Houston Black and Black Taylor clays showed similar results, with swelling of around 5% at 125 psf. Figure 2.5 presents the swell results.

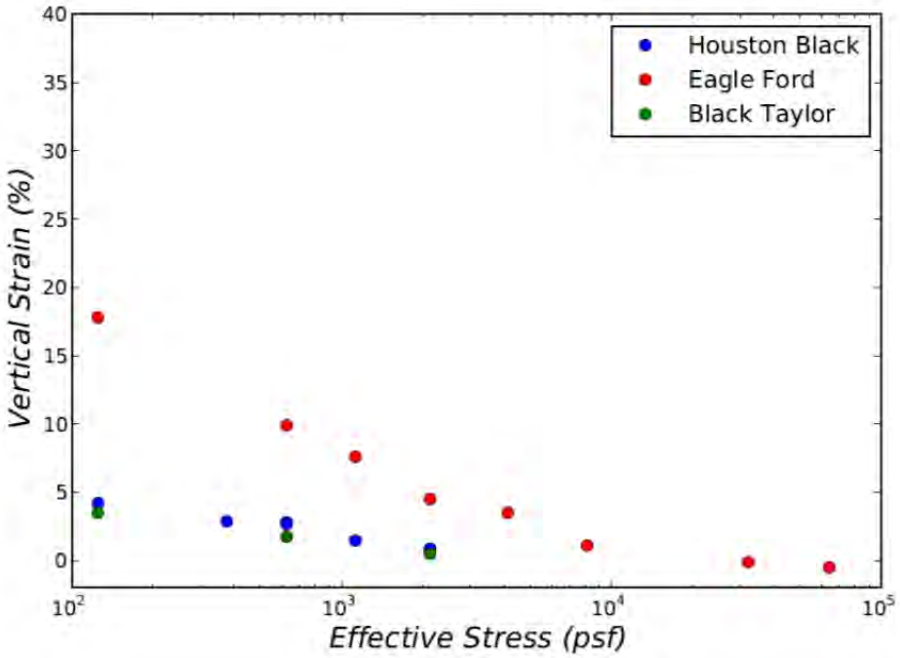

Figure 2.5: ASTM D4546 Swell Testing

Chapter 3. Equipment and Testing Procedures

Following the end of Project 0-6048 in August 2008, a centrifuge-based testing procedure was developed for the characterization of expansive soils, namely the direct measurements of vertical swell in a soil at a given effective stress. However, while the setup for Project 0-6048 was taken as an initial basis, the research team made numerous improvements to the centrifuge testing equipment and procedures. These alterations include the addition of a data acquisition system (DAS) that allows for a continual measurement of sample heights during testing, and changes in the testing procedures, specifically in specimen compaction.

3.1 Equipment Improvements

The addition of a DAS in the testing equipment has resulted in more accurate readings of the sample height during the testing procedure. The centrifuge originally used, the Fisher IEC EXD Thermo Explosion Resistant centrifuge, was replaced with the Damon IEC CRU-5000. Both centrifuges are operational with separate DAS. The Damon centrifuge was chosen because it allows more precise control over the g-level during testing and its Model 259 rotor has a six-cup capacity (four for soil samples and two for the DAS); Fischer's Model 277 rotor has only a four-cup capacity. The Damon centrifuge consists of a control board with a knob controlling RPMs, an RPM dial reading, a knob controlling temperature, a temperature dial reading, a knob controlling the timer, on/off power switch, start button, stop button, and a brake switch. Figure 3.1 displays the Damon Centrifuge as well as its control board. Figure 3.2 displays the Fisher Centrifuge as well as the inside portion of the centrifuge with its Model 277 rotor.

Figure 3.1: Damon IEC CRU-5000 Centrifuge and Control Board

Figure 3.2: Fisher IEC EXD Thermo Resistant Centrifuge and Model 277 Rotor

The metal buckets within the centrifuges each have an inner diameter of 2.5 inches, a usable inside depth of 4.5 inches, and a distance from the center of rotation to the base of the sample of 6.5 inches. The permeameter cup fits within the metal buckets and has four major components: the top cup, cup base, two porous disks with diameters equal to 2.25 inches, and two filter papers. The bottom porous disk is used as a base for the soil compaction, whereas the top porous disk sits on top of the sample to provide an even distribution of overburden stress from small washers. The total cup has a height of 4.5 inches, outside diameter of 2.49 inches, and inside diameter of 2.25 inches, and an air vent along the side of the cup. The original permeameter caps are no longer used during these tests as the effects of evaporation during the testing procedure are addressed by taping the top cap to the metallic cup. The biggest improvement in the test equipment comes from the addition of a DAS consisting of a battery housing unit with three batteries, a linear position sensor (LPS) for each of the permeameter cups (attached by a pair of screens) that monitors the height displacement of the compacted sample, a JeeNode (Version 6) Arduino along with the analog-to-digital converter (ADC), and an accelerometer that measures the g-level experienced by the test specimen. These components are displayed in Figure 3.3.

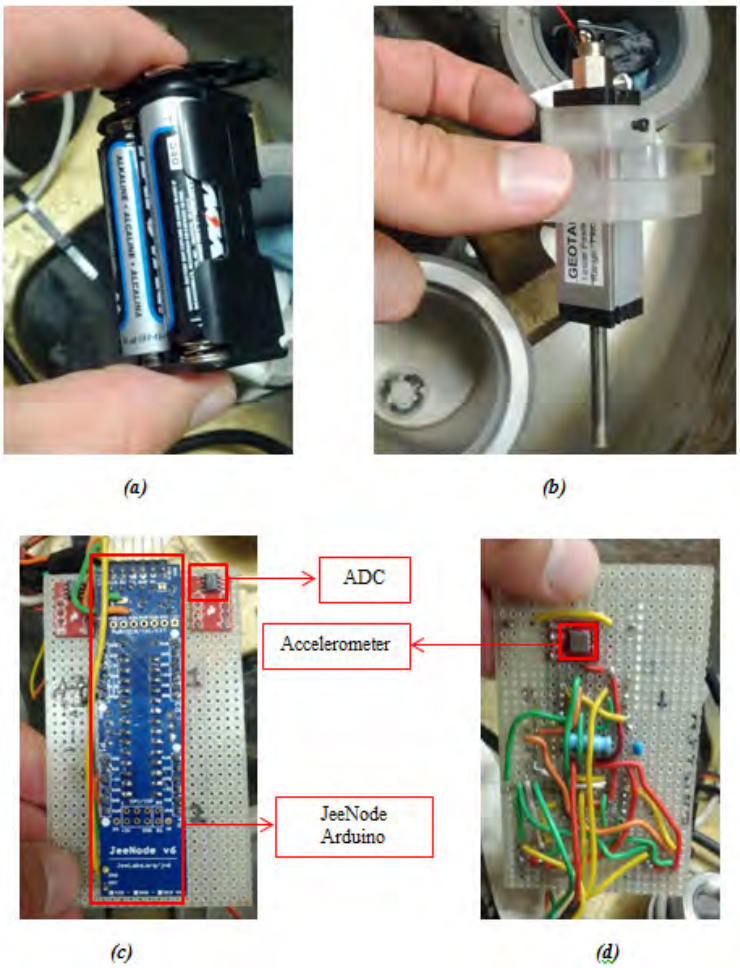

Figure 3.3: Major Components of the Data Acquisition System: (a) Battery Housing Unit with AA Batteries (b) Linear Position Sensor (c) JeeNode Arduino and Analog-to-Digital Converter (d) Accelerometer

The JeeNode Arduino contains a programmable microchip that controls and interfaces with the other DAS components through serial communication (RS232) and acts as the brain of the DAS, containing and running the program code to interface with the ADC. The Arduino sends a signal, notifying the ADC to take a reading from the LPS and the accelerometer. The ADC converts the LPS reading a voltage to a digital reading and sends it back to the Arduino along with the digital reading from the accelerometer. The internal JeeNode Arduino, housed within one of the centrifuge buckets, communicates the readings to an external JeeNode Arduino located outside of the centrifuge, via wireless radio. The external Arduino transfers the readings to the Labview program through a USB connection between the Arduino and the computer. The Labview program is then able to transform the readings into specimen heights, and the data is written in a text file that is converted via a Python script into the height of the sample and gives the g-level for each reading. **Therefore, the changes in the testing equipment lie mainly with the addition of the DAS and LPS** as well as the change from the Fischer to the Damon.

3.2 Improvements in Testing Procedure

The improvements in the testing procedure lie mainly in the changes for compaction and reading of the sample height as well as the way that swell is calculated. Appendix A details the testing procedures, providing photographs of the steps followed. This section summarizes the changes implemented, which dealt with sample compaction, height measurement, and the changes attending the addition of the DAS.

In the initial preparation of a sample, a calculated mass of soil (incorporating the target water content and relative compaction) is added to the cup and compacted using a thumb to create a soil structure that is strong enough to resist the kneading compactor. The kneading compactor is then used to get the soil structure within 0.02 inches of the soil. Note that the kneading compactor has a small surface area, creating an uneven surface on the top of the specimen. Therefore, the research team improved the testing procedure via use of a large diameter compactor and rubber mallet that creates an even surface. The large diameter compactor is placed flush against the cup walls and gently tapped with the rubber mallet. The cup is rotated 45° until a full 360° rotation has been completed. However, soil will accumulate along the inner diameter of the top cup during this compaction and a dental hook is used to move the soil stuck to the sides of the cup back into the cup, where it is re-compacted using the kneading compactor. The process is repeated until the surface of the soil is at or within +/- 0.001 of the target height at the center of the soil. Measurements are constantly taken after each step of the compaction at the middle and four reference points (top, right, bottom, left). Note that this approach of measuring the surface differs from the original approach as no water is added or suctioned off to determine the height of the sample because the small metal plate allows the researchers to take an average measurement of the inherently uneven soil sample surface. After the sample is compacted, the top filter paper and porous disk is added, along with washers for the seating load and compression cycle overburden as well as the washers for the overburden stresses to be applied during the testing procedure. These washers are stacked and placed in the center (in contrast to the previous testing methods, in which washers were distributed into three piles. Note also that the previous testing approach added water after adding the washers; the cups were then placed in the centrifuge, covered with caps to prevent evaporation, to run the test).

In the new testing procedure with the DAS, the assembled cups are then placed in the centrifuge, and the LPS is carefully placed such that it does not land on the washer but goes in the middle of the porous disk. The LPS is secured to the top of the cup using a piece of electrical tape to ensure its stability during the test. The Labview program is activated by pressing the Run button on the control screen (depicted in Figure 3.4).

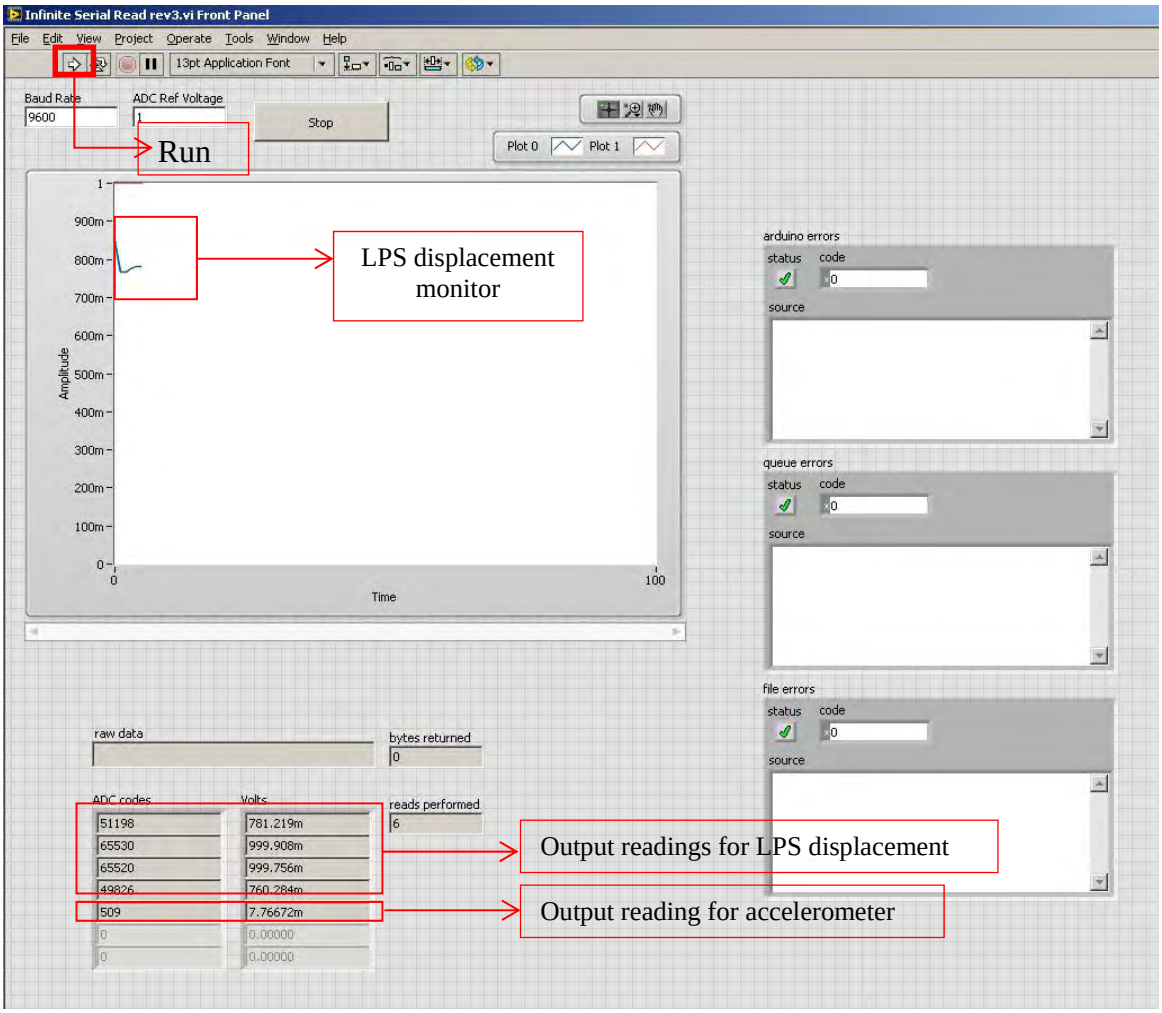

Figure 3.4: Screenshot of Labview Monitoring a Centrifuge Swell Test

These program functions and visuals are consistently used and monitored with every centrifuge test: the RUN function, STOP function, ADC reference voltage, LPS amplitude monitor, the LPS displacement output readings in ADC codes and voltage, and the accelerometer readings in ADC codes and voltage. The RUN and STOP functions begin and end the program's receipt and recording of data coming from the LPS and accelerometer within the centrifuge. The ADC reference voltage is used to scale the ADC reading and is set at 1.0 for this testing setup. The amplitude monitor shows the plot of the LPS output data, which indicates whether the sensor is displacing downward due to the sample compressing, or upward due to the sample swelling. The bottom right of the screenshot displays the ADC code and voltage readings from the LPS and accelerometer. One LPS displacement reading consists of one ADC code and one voltage. For the swell test corresponding to the screenshot in Figure 3.4, four LPS sensors are monitoring the displacement of four test specimens, with each LPS output reading consisting of an ADC code and voltage. The last pair of cells displays the ADC code and voltage for the accelerometer reading. In order to verify whether the target g-level has been reached, the ADC code from the accelerometer is closely monitored during the compression/decompression cycles and at the start of centrifugation where the ponded water begins to infiltrate the soil. Using a calibration

equation, the ADC code corresponding to the target g-level is computed, and the RPM dial gauge on the centrifuge is adjusted until the output ADC code reading is +/- 2 of the target ADC code.

The soil sample is then tested in the centrifuge environment and run through a seating load and a compression cycle. The seating load consists of raising the g-level in the centrifuge to between 2–3 g's and allowing the compression of the soil at a low seating pressure. This cycle is consistent with the seating load applied prior to the compression cycle in the standard swell test.

The compression cycle consists of raising the soil (without access to water) to the specified RPM and g-level for several minutes and then stopping the centrifuge. This allows the measurement of the compression due to the increased load during centrifugation. In cases where field samples are characterized, g-level should be selected to replicate desired field stresses. For compacted samples such as the ones reported in this report for general characterization of the soil, specimens should be tested at g-levels of 5, 25, and 200. These g-levels produce effective stresses in samples ranging from approximately 10 psf up to 2000 psf, which is representative of the stress range typical to the active zone for expansive clays. Figure 3.5 illustrates the ranges in stress seen in centrifuge samples at g-levels 5, 25, and 200 along with the stress range for a 15 foot layer of with a 10 psf pavement overburden.

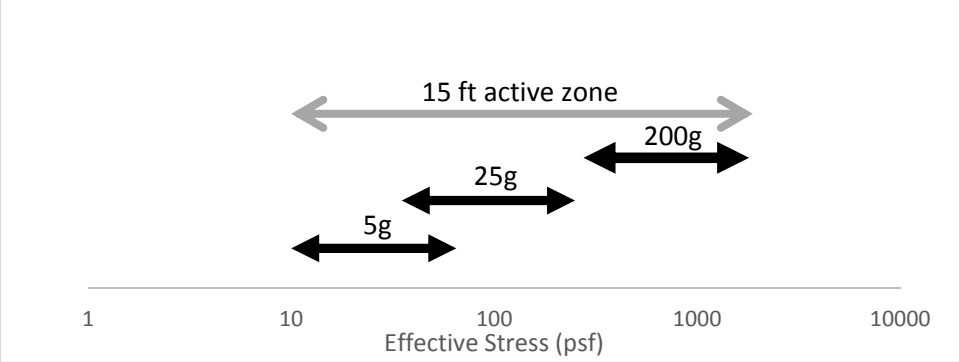

Figure 3.5: Stress Ranges of Select G-Levels and Active Zone

After compression cycle, the soil is removed from the centrifuge, and the overburden washers are removed. (These washers weigh approximately 25.65 grams, which is meant simulate half the weight of the water added in the next step). Then 51.3 grams of water is added to the cups, and the cups are immediately returned to the centrifuge. The centrifuge is then run again, and allowed to swell for 42–48 hours. Primary swelling of the sample is typically completed with one day, and the sample is allowed to run for extra time to ensure that secondary swelling has begun. After the test is completed, the cups are removed from the centrifuge, and the mass of the cup and cup base with water are then measured. Final sample heights are again measured to determine the final swell in comparison to that measured in the centrifuge. The soil is then extruded and placed on a metal tray that will be put in an oven to measure the gravimetric water content of the soil. This step concludes the testing process. The improvements in the testing procedure include

- adding a large diameter compactor to create a flatter surface on the soil sample,
- changing the compression cycle using the DAS and LPS to ensure both a true seating load cycle and a compression cycle for the required g-level, and
- using DAS and LPS in testing to obtain in-flight measurements of soil sample height.

3.3 Summary of Improvements in Testing Equipment and Procedure

The primary improvement in the testing equipment and procedure was the addition of the DAS and LPS that capture soil swelling during the test, obviating the need to stop the test. Thus, the researcher team can accurately analyze the process of soil swelling and water absorption. Further, the true swelling of the soil can be determined—earlier procedures required stopping the centrifuge, thereby removing the loading condition and allowing the soil to swell more rapidly in the time removed from the centrifuge to the mounted dial gauge. Also, small changes in the compaction procedures, such as the addition of a large diameter compactor to create a much flatter soil surface, allowed for a more precise and level surface for the porous disks to sit on. Finally, the change of the compression cycle—setting the seating load compression at 2 to 3 g's and the full compression at the required g-level—allows for consistent loading conditions prior to the addition of water, thus providing uniform compression prior to swelling.

Chapter 4. Analysis of Centrifuge Results

The analysis of swell results from centrifuge tests requires a unique approach because each sample is subject to a wide range in stresses. The range in stresses is a result of the high g-level induced during testing; the g-level increases the unit weight of the soil, resulting in a significant range in stresses across the sample. Two analysis methods will be discussed in this report. Both methods require the effective stresses to be calculated in centrifuge samples.

4.1 Calculating Effective Stresses in Centrifuge Samples

Two methods may be used to calculate the effective stress in centrifuge samples. The first, robust method allows the entire stress profile of centrifuge samples to be calculated. The second, simpler method calculates only effective stresses at the top and base of the sample, which is all that is required for the analysis methods discussed in this chapter.

4.1.1 Robust Method

To analyze the centrifuge test results, the research team developed a framework to calculate the elevated stresses in centrifuge samples. It is possible to calculate soil pressures by considering that the unit weight of a soil under centrifugal acceleration is

$$\gamma_c = \rho\omega^2 r$$

where ω is the rotational velocity of centrifuge and r is the radius from the center of rotation to the soil. The unit weight of soil changes with the centrifuge radius and therefore soil pressures must be calculated by integrating across the centrifuge radius such that the pressure from soil above any radius is defined as

$$p(r) = p_t + \int_{r_t}^{r} \rho_s \omega^2 r \, dr$$

where p_t is the pressure at the top of the soil specimen due to water head or overburden and r_t is the centrifuge radius at the top of the soil sample. This relationship can be used to define the total stress in a soil specimen.

The pore water pressures in centrifuge samples were determined by assuming steady state flow, saturation of samples, and Darcian flow. The fluid potential was calculated as

$$\Phi_c = \frac{1}{2}\omega^2(r_0^2 - r^2) + \frac{P(r)}{\rho_w}$$

where r_0 is the radius of the sample base (taken as the datum). Given a centrifuge discharge velocity of

$$v_c = -\frac{k_s}{g}\frac{\delta\phi_c}{\delta r}$$

where g is the gravitational constant, the fluid potential formula can be differentiated and the discharge velocity substituted. After integration the pore pressure was found to be

$$P(r) = \frac{1}{2}\rho_w \omega^2 r_0^2 + C_1 r_0 + C_2$$

The two constants C_1 and C_1 were determined by imposing boundary conditions ($P(r_0) = 0$, $P(r_t) = P_1$, the applied pressure head). The full derivation can be found in Section 6.3.2 of Plaisted (2009).

The resulting stresses from these derivations have been plotted for a 2 cm tall (.79 inch) specimen. The base of the specimen is at a centrifuge radius of 16.51 centimeters (6.5 inches). For this specimen height and g-level, the stresses are nearly identical to a linear approximation. The linear approximation assumes the entire specimen is at a g-level equal to the g-level calculated for a radius at mid specimen height. The maximum error due to a linear approximation was less than 1% of the more accurate parabolic stress distribution determined using the more robust method accounting for a g-level varying with radius. Figure 4.1 illustrates the sample stresses.

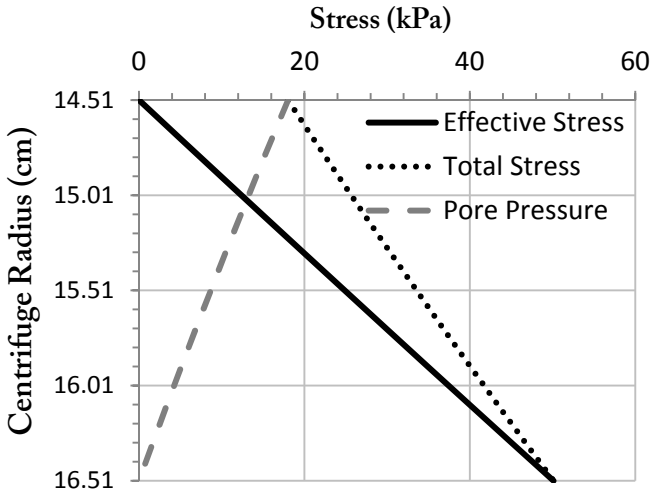

Figure 4.1: Stresses in a Centrifuge Sample

4.1.2 Simplified Method

Both analysis methods proposed in this report assume a linear distribution of effective stresses in between the top and base of centrifuge samples. This allows the state of stress in a centrifuge sample to be fully defined by the effective stresses and the top and base the sample. A simplified procedure for calculating stresses at the top and base of specimens is described below. This procedure involves scaling the masses in the centrifuge by the g-level at the center of the mass.

The effective stress at the top of specimens is solely the result of the applied overburden mass. The overburden mass is submerged so the applied mass must be scaled down to the submerged mass. Therefore the effective stress at the top of specimens can be calculated as Equation 4.1:

$$\sigma_t' = \omega^2 r_{ob} \frac{(\rho_{ob} - \rho_w)}{\rho_{ob}} m_{ob} \frac{1}{A} \tag{4.1}$$

where ω is the rotational velocity of centrifuge, r_{ob} is the radius from the center of rotation to the center of the overburden mass, ρ_{ob} and ρ_w are the density of the overburden and water

respectively, m_{ob} is the mass of overburden, and A is the area of the centrifuge sample. It is usually valid to assume that r_{ob} is equal to r_t as the overburden mass is usually applied by washers with negligible thickness.

The effective stress at the base of the sample is equal to the total stress, as the base of the sample is a freely draining boundary with pore water pressure equal to zero. The total stress can be calculated by adding the stress increase due to the applied overburden mass, the ponded water on top of the sample, and the saturated soil mass together such that we get Equation 4.2:

$$\sigma_b' = \frac{\omega^2}{A}\left(r_{ob}\frac{(\rho_{ob}-\rho_w)}{\rho_{ob}}m_{ob} + r_w m_w + r_s m_s\right) \tag{4.2}$$

where m_w and m_s are the mass of the water and saturated soil mass respectively and r_w and r_s are the centrifuge radiuses at the center of the water and soil layers. These equations provide a quick and accurate method to calculate the effective stresses at the top and base of centrifuge samples and the resulting values can be directly used in the analysis methods proposed in this report.

4.1.3 Concept of Equivalent Stress

The two proposed analysis methods are both based on the concept of "equivalent stress." For a given stress-strain relationship, $\varepsilon(\sigma')$, the total strain for a sample with stresses ranging from σ_t' to σ_b' can be calculated as Equation 4.3:

$$\varepsilon_{ave} = \frac{\int_{\sigma_t'}^{\sigma_b'} \varepsilon(\sigma')}{\sigma_b' - \sigma_t'} \tag{4.3}$$

The equivalent stress is the stress value that would result in the same strain value that was calculated using Equation 4.3 but by using a single stress rather than a range in stresses. The equivalent stress can be calculated as Equation 4.4:

$$\sigma'_{equiv} = \varepsilon^{-1}(\varepsilon_{ave}) \tag{4.4}$$

In order for Equation 4.3 to be valid, a linear distribution of effective stress across the sample must be assumed. The distribution has been shown to actually be better represented by a polynomial distribution (Plaisted 2009), but errors between the two distributions were found to be less than 1% and the errors due to the assumed distribution to be less than 0.25% (Plaisted 2013). If the equivalent stress is calculated for a centrifuge sample, the swell measured for the sample can be related to the equivalent stress and results analyzed similarly to results from standard swell tests.

4.2 Representative Stress Method (Method 1)

The representative stress method was developed in order to approximately determine the equivalent stress of a centrifuge test using only the results from a single centrifuge test. The method is based on the assumption that the swell-stress relationship is log-linear across the range of stresses of a single sample.

In order to calculate the equivalent stress, a log-linear swell-stress curve is assumed as shown in Equation 4.5:

$$\varepsilon = A \ln(\sigma') + B \tag{4.5}$$

The average strain across a range of stresses can be calculated using Equation 4.3. The equivalent stress cannot be directly calculated as the coefficients *A* and *B* are unknown. However, the results indicate that the location of the equivalent stress relative to the stress range was independent of the coefficients of the assumed log-linear relationship. Therefore, if the ratio of stresses at the base and top of the specimen is as shown in Equation 4.6:

$$SR = \frac{\sigma_b'}{\sigma_t'} \tag{4.6}$$

and the interpolation value is defined as shown in Equation 4.7:

$$IV = \frac{\sigma_t' - \sigma_{equiv}'}{\sigma_b' - \sigma_t'} \tag{4.7}$$

then Equation 4.3, 4.6, and 4.7 can be substituted into Equation 4.4, and the terms rearranged and reduced in order to produce a relationship between the stress ratio (SR) and the interpolation value (IV) to create Equation 4.8:

$$IV = \frac{\frac{1}{e} SR^{\left(\frac{1}{SR-1}+1\right)} - 1}{SR - 1} \tag{4.8}$$

The resulting function is shown in Figure 4.2 over a range of stress ratios typical for centrifuge testing. Using Figure 4.2 or Equation 4.8, the interpolation value can be calculated for a single centrifuge test. By rearranging Equation 4.7, the equivalent stress can be determined from the interpolation value, as follows in Equation 4.9:

$$\sigma'_{equiv} = (\sigma_b' - \sigma_t')IV + \sigma_t' \tag{4.9}$$

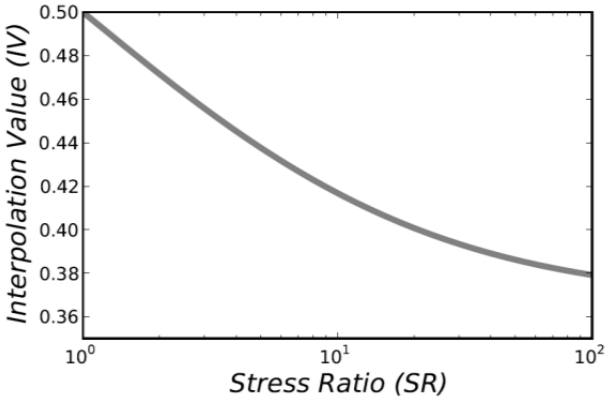

Figure 4.2: Stress Ratio and Interpolation Value

The representative stress method was conducted for a set of tests conducted at g-levels of 5, 25, and 200 and the results are included in Table 4.1. The results show a well-defined trend between the equivalent stress and swell, which will be discussed later.

Table 4.1: Representative Stress Results

Swell (%)	σ_t' (psf)	σ_b' (psf)	SR	IV	σ_{equiv}' (psf)
8.99	32.5	219	6.59	0.43	908.8
8.58	32.6	219	6.54	0.43	909.9
18.87	268	1760	6.73	0.43	112.2
18.42	269	1760	6.72	0.43	112.3
29.81	9.03	62.4	6.91	0.43	31.84
31.12	9.02	62.7	6.94	0.43	31.93

4.3 Curve Fitting Method (Method 2)

The curve fitting method is used to solve for the function coefficients that result in the least error between the measured swell in centrifuge tests and the predicted swell based on the fitted swell function. The fitted function can then be used to accurately calculate the equivalent stress for each centrifuge test. While the procedure is similar to that used in general curve fitting, adjustments were made since the curve is being fit to data over a range of stresses rather than a point.

This method requires data from at least three centrifuge tests. A function is then chosen with baseline coefficients. The average swell is calculated for the range in stresses of each test using Equation 4.3 and the assumed function $\varepsilon(\sigma')$. Calculating the average will likely require numerical integration unless a simple function is found that fits the data.

The calculated average swell is compared with the measured swell for each test and total error calculated using the least squares method to result in Equation 4.10:

$$Error = \sum_{i=0}^{n} (\varepsilon_{ave,i} - \varepsilon_{measured,i})^2 \quad (4.10)$$

Coefficients are refined and the process is repeated using the updated coefficients until the minimum error is found. Powell's method (SciPy 2013) is used in order to find minimum error of the function.

The process of determining the function to be used can be achieved in two ways. The first approach is to complete the analysis of all testing results using the Representative Stress Method in Section 4.2. The results from the representative stress method are plotted and a function is chosen that matches the general shape of the relationship found between swell and stress in the plotted data.

The second approach is to pre-select a variety of functions that typically represent well the relationship between swell and stress for expansive soils. The curve fitting method is then performed for all of the selected functions and the function with the lowest error is chosen.

Three functions that have been found to fit well swell-stress curves are listed as Equations 4.11 through 4.13. The procedure listed above was completed for each function using a Python script to automate the process. The resulting best-fit coefficients and the corresponding least-squares error are included in Table 4.2.

$$Swell(\sigma') = A \ln(\sigma') + B \quad (4.11)$$

$$Swell(\sigma') = A \ln(\mathrm{B} \ln(\sigma') + 1) + C \quad (4.12)$$

$$Swell(\sigma') = \frac{A}{\ln(B\sigma' + 1)} + C \quad (4.13)$$

All three functions provide a good correlation between effective stress and swell. The best-fit coefficients and errors for each equation are included in Table 4.2. The log-linear function performs worst, but for practical purposes would most likely be satisfactory for the small ranges in stress typical of the active zone of a soil profile. Equation 4.13 provides a very accurate representation of the swell-stress relation and was consistently found to be the best fit of the three functions for all data sets evaluated. Once the best fit function has been found, the equivalent stresses for each test can be calculated using Equation 4.3 and 4.4. The best-fit curve has been plotted in Figure 4.3 along with equivalent stresses determined from the resulting function and the range of stresses for each sample.

Table 4.2: Curve Fitting Results

Equation	A	B	C	Error
(4.11)	-7.55	56.39	N/A	39.5
(4.12)	-107.5	53113	322.7	14.2
(4.13)	128.8	0.714	-11.15	1.12

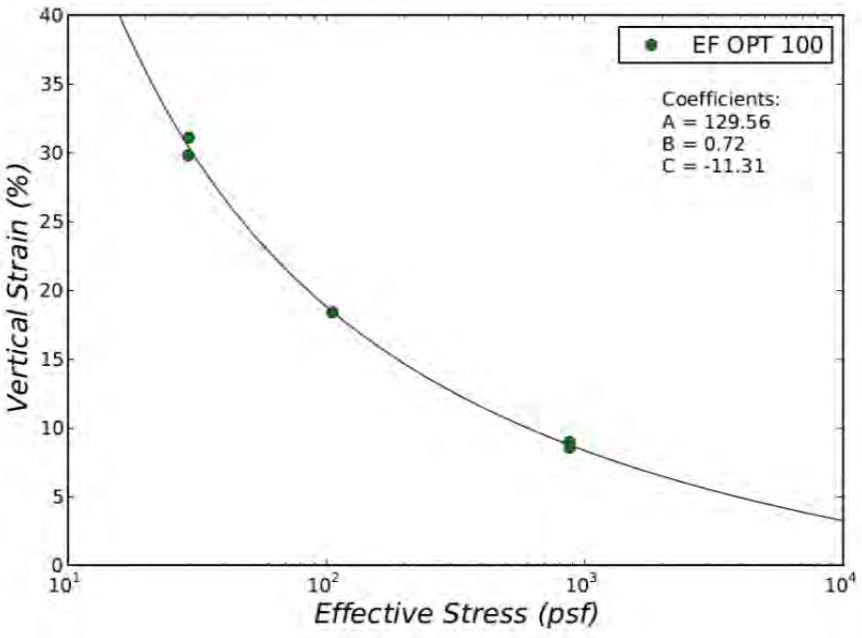

Figure 4.3: Results from Curve Fitting

Chapter 5. Centrifuge Test Results

5.1 Scope and Results on Swelling

Five soils were tested in this project: the Eagle Ford shale, Houston Black clay, Black Taylor clay, Tan Taylor clay, and Soil 5. The baseline conditions selected were that of optimum moisture content of a soil compacted to a density equal to 97% relative compaction from the standard proctor test. For example, the Eagle Ford baseline condition consisted of a soil that had a moisture content equal to 24%± 0.5% and a dry unit weight of 14.34 kN/m^3. In order to conduct a parametric evaluation, the moisture content of a soil was varied at three moisture contents: the optimum moisture content and ±3% from the optimum moisture content. The three relative densities used in compaction were 94%, 97%, and 100% of the dry density as determined by the standard proctor test. The moisture content was varied in order to compare the results of the swelling at the optimum water content as well as behavior below and above the optimum moisture content. We implemented this variation after seeing a noticeable peak in the swelling of a clay around the optimum moisture content with a decrease in swelling at both moisture contents above and below the optimum moisture content for the Free Swell tests. This variation was implemented in accordance with the scope and work plan at the beginning of the project.

To generate a range of effective stress, g-levels of 5, 25, and 200 g's were selected in order to generate the stress-swell curves. These g-levels represent approximately 30, 100, and 1000 psf.

The testing program involved 183 samples. While the research team is continuing to test, this is a "final" report of the number of tests run. The vast majority of tests completed were on the Eagle Ford shale; the Tan Taylor and Soil 5 were tested the least. Note that the majority of the samples were tested at the optimum moisture content. Appendix B contains the technical data from each test. Table 5.1 breaks down the tests in terms of g-level and initial moisture content.

Table 5.1: Breakdown of Centrifuge Tests and Samples

Soil	5g	25g	200g	DOPT	OPT	WOPT	Total
Eagle Ford	23	34	14	21	46	6	73
Houston Black	24	14	10	8	35	5	48
Black Taylor	16	15	12	6	32	5	43
Tan Taylor	10	5	0	4	3	8	15
Soil 5	1	2	1	0	4	0	4
All Soils	74	70	37	39	120	24	183

Table 5.2 contains the average swelling data at the baseline conditions for the three most tested soils—the Eagle Ford, Houston Black, and Black Taylor—for each of the tested g-levels.

Table 5.2: Baseline Conditions for the Test Clays

Soil	w, opt (%)	Target Dry Unit Weight, (kN/m^3)	5g Swelling (%)	25g Swelling (%)	200g Swelling (%)
Eagle Ford	24	14.79	24.68	15.65	7.26
Houston Black	25.5	14.28	6.13	5.34	1.46
Black Taylor	23.3	14.28	3.92	2.65	2.26

The most highly plastic soil, the Eagle Ford shale, has the highest average swelling per test, which is to be expected. Also, interestingly enough, the Houston Black clay does have higher average swelling values for the 5-g and 25-g tests than the Black Taylor, which is also to be expected as it has a higher PI than the Black Taylor clay, but has a lower swelling value for 200 g's. However, neither clay has nearly the swelling potential of the Eagle Ford soil.

For each test, the data recorded from the DAS is the change in height of a soil at a specified time interval. From this data, the swelling of a sample can be measured continuously throughout the test, and a swell versus time curve can be generated. A typical swell-over-time curve is shown in Figure 5.1. Note that the conditions for this curve involve an Eagle Ford clay run at baseline conditions.

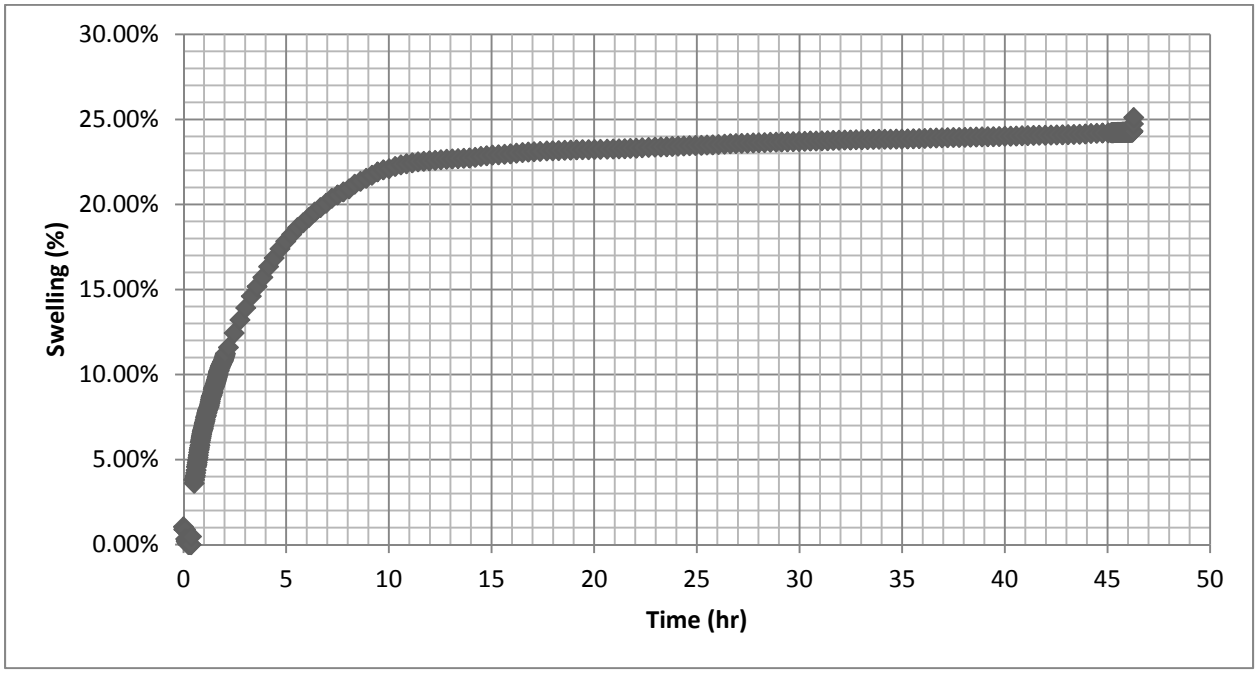

Figure 5.1: Swelling vs. Time for an Eagle Ford Baseline Test Specimen

As the figure illustrates, the first portion of the swelling curve is where the primary swell occurs in which the void ratio of the soil dramatically changes as the water enters the voids. This stage typically takes around 10 hours, until the swelling hits an inflection point, and then continues through to a secondary swelling at a much decreased rate. Therefore, the inflection point is taken as the swelling of a soil at a given pressure in order to only account for the primary swelling of a soil. This approach was used to define the swelling of a sample for every test. Also,

considering the shape of the curve for the other soils is not as smooth at this transition, the general portions of the test, i.e., the location of where the primary swelling occurs and time to reach the end of primary swelling, are slightly inconsistent between soils due to differences in the soil structure and composition.

Data from these tests are presented in Appendix B, with a breakdown of the number of tests by moisture and compaction conditions for the Eagle Ford, Houston Black, and Black Taylor included as well. Note that Figure 2.2 contains the basic soil identification characteristics.

5.2 Swell-Stress Curves

The swell-stress curves were calculated for the three main soils for which a large suite of tests were conducted using the curve fitting method previously described. The three soils were the Eagle Ford, Black Taylor, and Houston Black clays. The resulting curves are shown in Figure 5.2. The Eagle Ford clay shows significantly higher swelling potential than both the Black Taylor and Houston Black. The Black Taylor and Houston Black clays show similar swelling potential with the Black Taylor resulting in a slightly higher swell-stress curve.

Curves based on samples with varied compaction moisture and density were also calculated for the Eagle Ford, Houston Black, and Black Taylor clays. The results are included in Figures 5.3 through 5.8. The results for compaction moisture content showed the swell decreasing with increasing compaction water content. Likewise, the compaction density curves showed higher swell for samples compacted at higher densities for the Eagle Ford and Black Taylor. Both of these results agree with previously reported trends for swelling potential and compaction conditions.

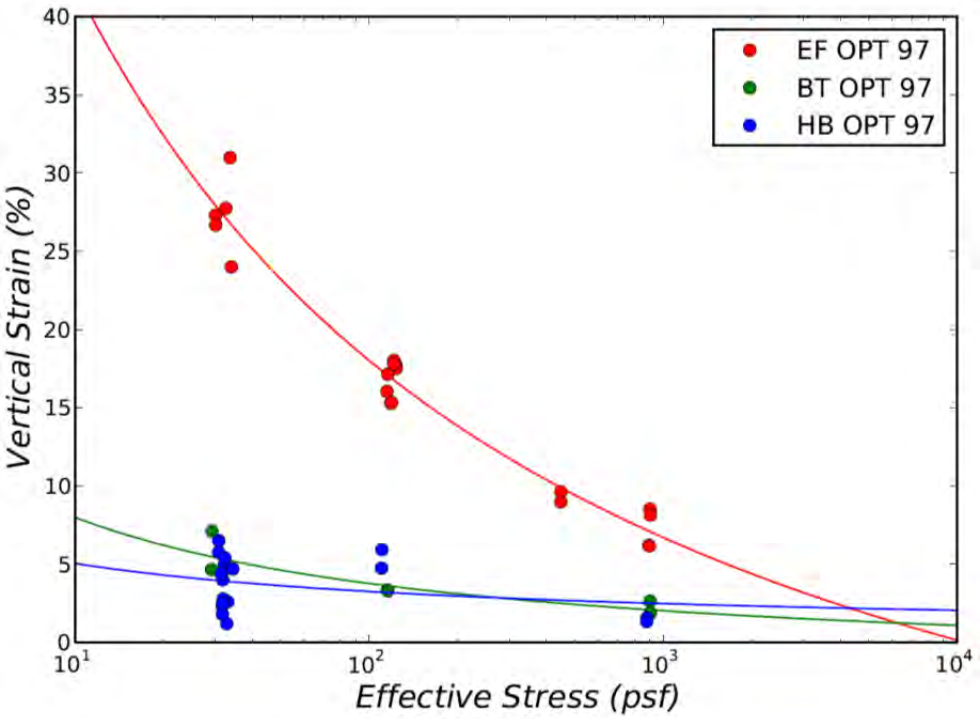

EF = Eagle Ford; BT = Black Taylor; HB = Houston Black

Figure 5.2: Baseline Curves

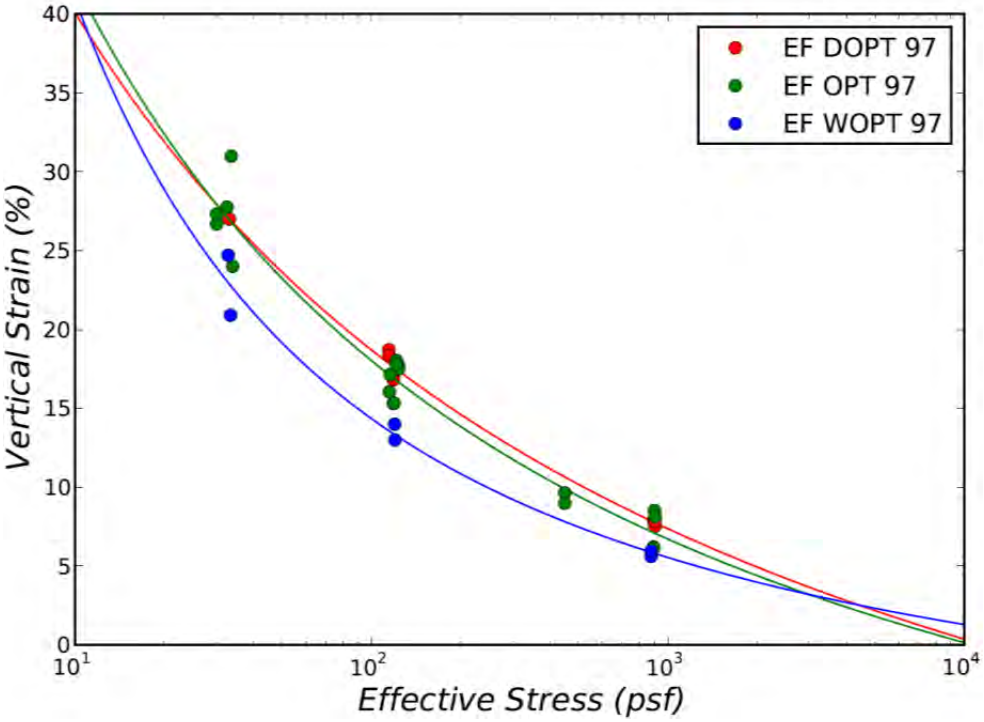

Figure 5.3: Compaction Moisture (Eagle Ford)

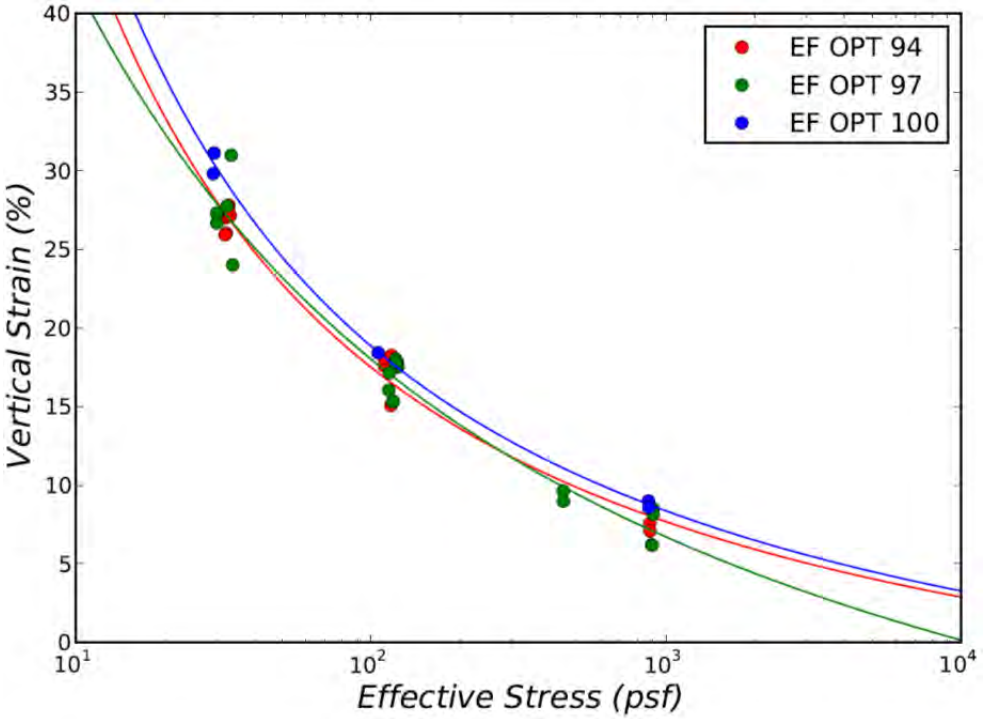

Figure 5.4: Compaction Density (Eagle Ford)

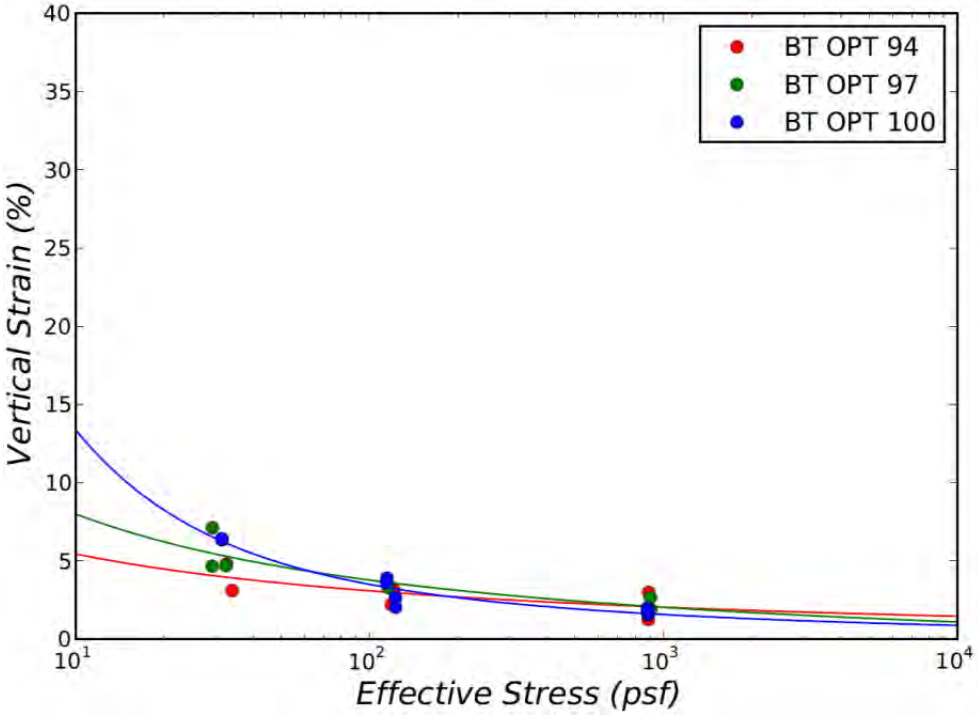

Figure 5.5: Compaction Density (Black Taylor)

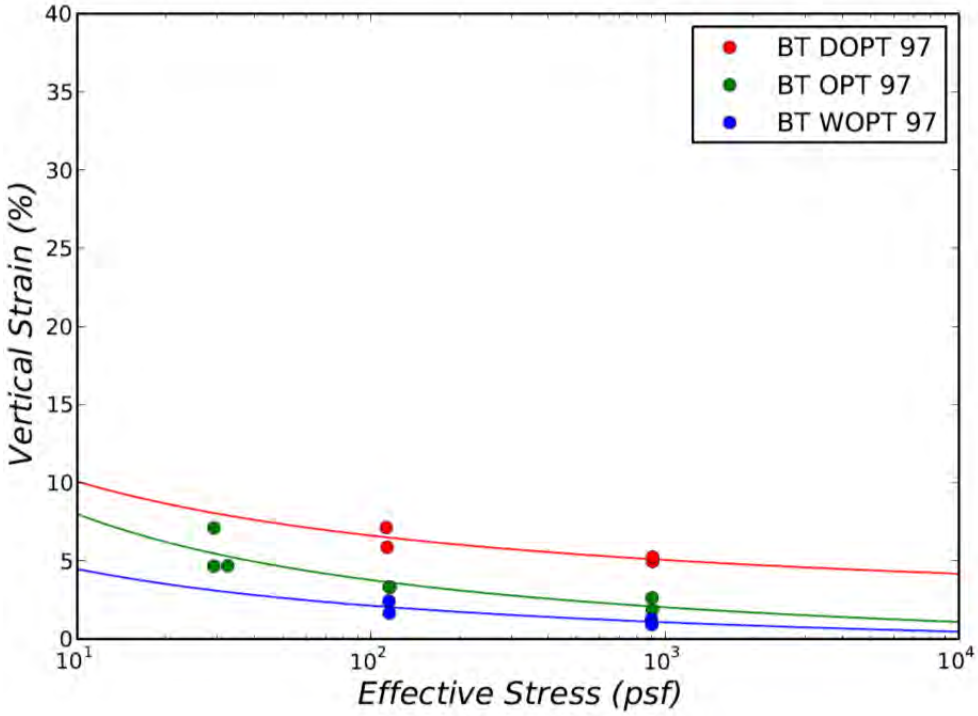

Figure 5.6: Compaction Moisture (Black Taylor)

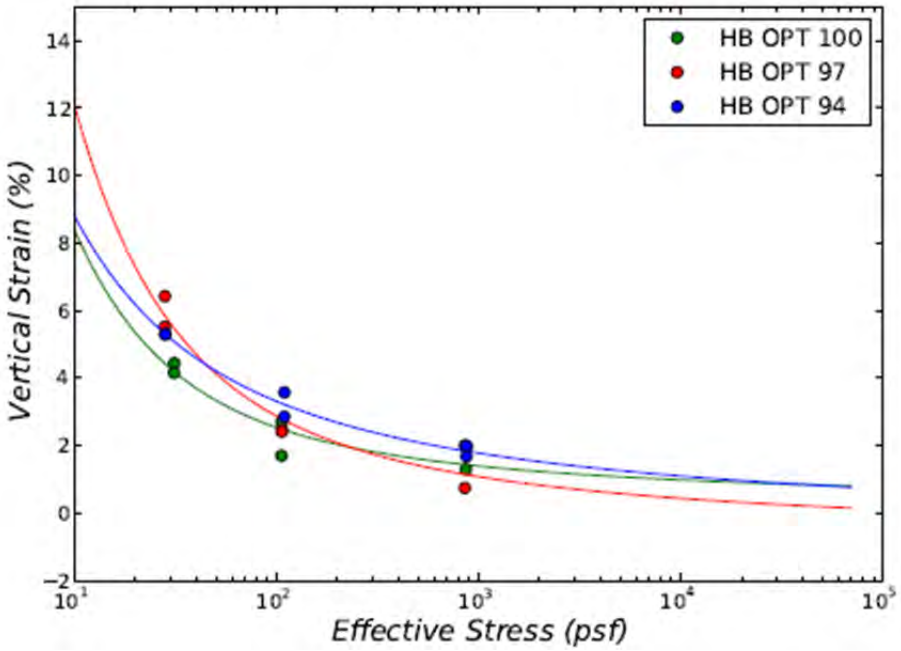

Figure 5.7: Compaction Density (Houston Black)

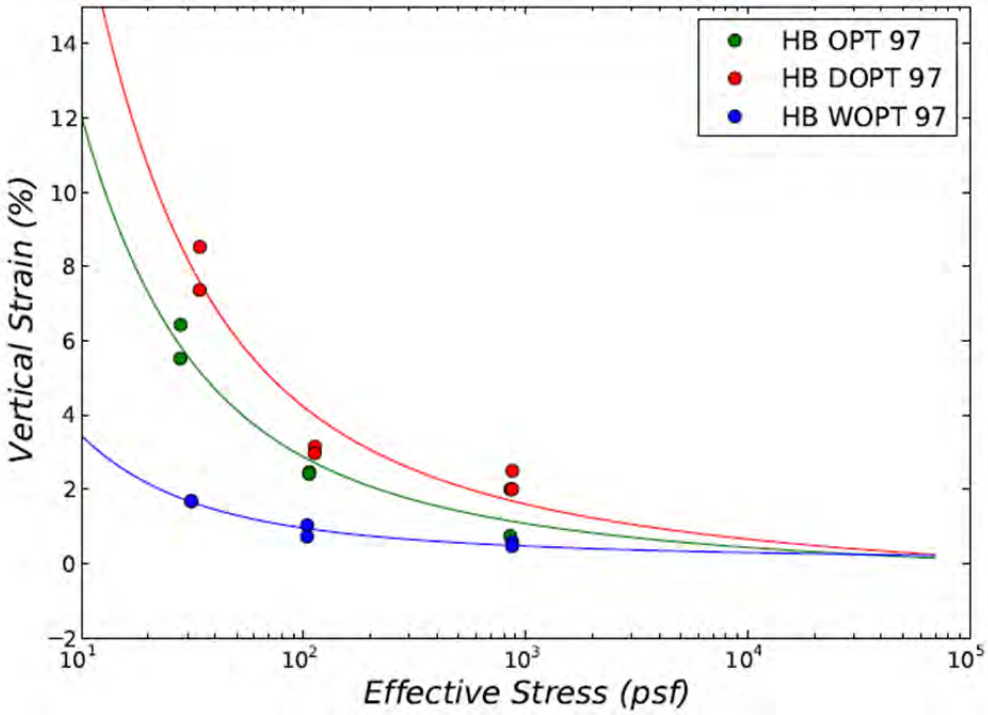

Figure 5.8: Compaction Moisture (Houston Black)

5.3 Comparison with Standard Swell Test Results

The results obtained from the centrifuge testing procedure were compared with the standard swell test results using the same compaction density and water content. The results were analyzed using the curve fitting method and the equivalent stresses for each centrifuge test were calculated based on the resulting curve. The centrifuge results showed an excellent correlation with the standard swell test results for all three soils. The results are included in Figures 5.9–5.11.

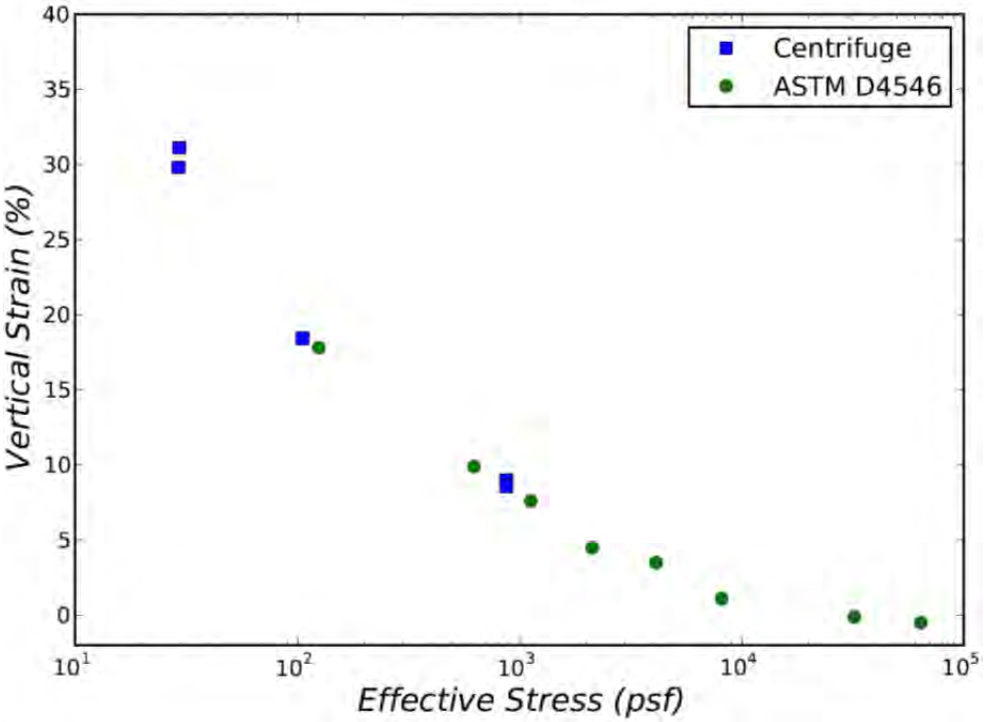

Figure 5.9: Centrifuge vs. Standard Results (Eagle Ford)

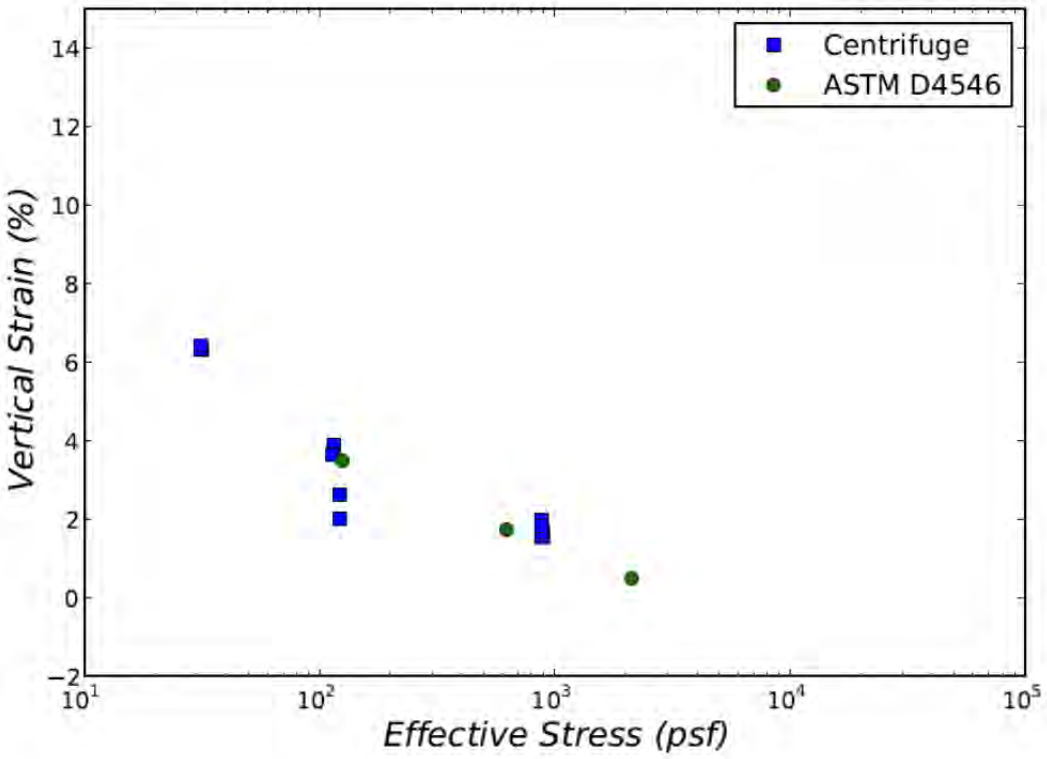

Figure 5.10: Centrifuge vs. Standard Results (Black Taylor)

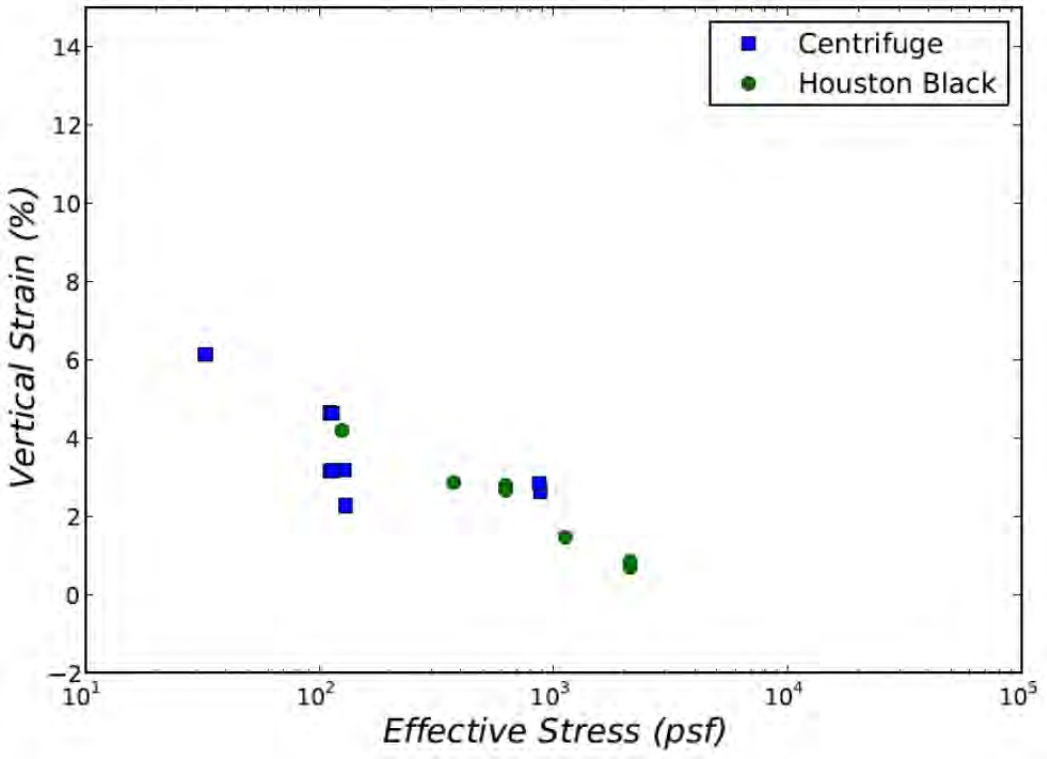

Figure 5.11: Centrifuge vs. Standard Results (Houston Black)

Chapter 6. Preliminary Approach for Refinement of PVR Methodology

TxDOT's current procedure consists of a modified version of McDowell's 1959 method, with the modification coming in the form of a "free swell" conversion ratio. This method consists of correlating a soil's PVR with the soil's PI. However, this method does not provide site-specific calculations or data that incorporates actual testing of the soil present, which can lead to under-predicting a soil's vertical rise by approximately 50%. Therefore, a new method, Method 6048 (A), is proposed in which a database of swelling results from clays typically encountered in Austin can be used as a preliminary evaluation for locations.

Further, another method that uses the results from centrifuge testing can be used in order to determine the project-specific PVR, Method 6048 (B), can also be used in the final design of roadways to fully understand the swelling capacity of a particular site. This section outlines the methodology for both Methods 6048 (A) and 6048 (B), which are similar in their approach. Appendix C includes training material in form of a PowerPoint presentation that describes the methodology for both approaches as well as the current TxDOT standard. A comparison between methods is also illustrated via an example problem, illustrating the TxDOT PVR methods' ability to over predict a soil's ability to swell.

6.1 Method 6048 (A)

In order to use Method 6048 (A), a database of highly plastic, expansive clays in Austin should be available, which includes the swelling as a function of the density, or initial void ratio, of the clay as well as the initial moisture content. The five soil tested in this implementation project are currently available as a database, with the capacity of many more test within the future. In order to determine the swell, data from boring logs or inferred data from practical experience should be collected, namely the water content of the soil, void ratio, and soil type with depth. Other properties, such as index properties, grain size distributions, sulfate content, etc., can also be useful in fully characterizing a location. After the location is properly classified, the soil profile should be divided into sub-layers, typically equivalent to around 2 feet, and the effective stress at the top and bottom of each sub-layer should be determined. From there, the fully swollen void ratio (FSVR) should be determined for the range of stresses within the sublayer. The average FSVR can be taken in a number of ways:

- as the FSVR corresponding to the effective stress at the center of the layer (less accurate);
- as the FSVR corresponding to the log-average of the effective stress at the top and bottom of the layer; or
- as the average of the FSVR curve across the range of stresses in the layer (the most accurate approach, this requires integration).

The second or third alternatives described above are preferable as they are more accurate. Once the FSVR is determined, the difference between the current, or initial, void ratio and the FSVR should be calculated. If the FSVR is greater than the current void ratio, the PVR of the layer is taken as 0. This condition can occur for soils that are recently consolidated, which were

originally close to the FSVR, or those soils with stress histories that have raised the void ratio of the soil. The swell is then determined as follows:

$$Swell\ (\%) = 100\% * \frac{\Delta e}{1 + e}$$

After determining the swelling in each layer, the PVR of a layer is calculated by multiplying the swell by the thickness of each layer. The total PVR of the soil profile is determined by taking the sum of each of the layers. This method can generate a general idea of the expected amount of PVR for a given site, although the use of Method 6048(B) is highly recommended in order to properly characterize a site.

6.2 Method 6048 (B)

The methodology for Method 6048 (B) is similar to 6048 (A) in terms of the calculations but differs in the source of the experimental data, which comes from project-specific soils that are characterized by the centrifuge testing project. In order to use Method 6048 (B), undisturbed clay samples must be collected using Shelby Tubes in order to have soil samples to use in the centrifuge as well as data for other index properties of the clay layer. Once the sample is collected, tests at three different effectives stress, typically centrifuge tests at 5 g's, 25 g's, and 200 g's, must be run to generate the swell vs. effective stress for each layer. Note that the FSVR is not needed in this stage as the data can directly give the swelling curve. The procedure for the rest of the calculations remains the same as Method 6048 (A), as the swelling values are multiplied by the sublayers in order to get the PVR of the layer and summed up to get the total PVR. As such, this method generates the PVR for a project-specific soil that should be used in design calculations.

Chapter 7. Final Remarks

At the end of the implementation of Project No. 5-6048-01, the centrifuge testing program has proven successful in terms of developing a new procedure to calculate the PVR of a site both via an archive method and a project-specific method in which samples from a site can be tested to determine the stress versus swelling curve. The testing project has illustrated that the benefits of a centrifuge-based analysis consist of the following:

- Allows assessment of the direct relationship between a soil and its capacity to swell rather than depending on a correlation based on the plasticity index
- Time savings from being able to run multiple samples at the same time in a single test
- Tests can be run under various confining conditions
- Samples can come from reconstituted specimens, with potential to expand testing to take samples from the field

An important recommendation is to implement a testing procedure that can account for samples taken from undisturbed sites (in Shelby tubes) to accurately predict a site's PVR. Further, additional testing would be valuable to expand the database in order to complete the swelling versus stress curves for the initial soils at various moisture contents and density conditions, as well as for other soils found in the Austin District of TxDOT and other districts. Once more soils can be tested, as well as samples from the field, a direct comparison study between each of the methods can be conducted to verify the full benefit of the use of centrifuge technology in practice.

References

Allen, J., 2004, "Forced Ventilated Swell-Shrink Test for Potential Vertical Expansive Soil Movement." Thesis, Master of Science in Engineering, The University of Texas at Austin.

American Society of Testing and Materials, 2000, "Standard Test Method for Determining Unsaturated and Saturated Hydraulic Conductivity in Porous Media by Stead-State Centrifugation." ASTM D6527-00. West Conshohocken, Pennsylvania.

Bear, J., Dynamics of Fluids in Porous Media. Elsevier, New York, 1943.

Cinicoioglu, O., Znidarcic, D., and Ko, H., 2006. "A New Centrifugal Testing Method: Descending Gravity Test." *Geotechnical Testing Journal*, Vol. 29, No. 5, pp. 1–10.

Covar, A. P., and Lytton, R. L., 2001, "Estimating soil swelling behavior using soil classification properties." *Expansive Clay Soils and Vegetative Influences on Shallow Foundations*, ASCE Geotechnical Publication No. 115, American Society of Civil Engineers, Reston, VA, pp. 44–63.

Jones , D. E., and Holtz, W. G., 1973, "Expansive Soils – The Hidden Disaster," Civil Engineering, Vol. 43, no. 8, pp. 49–51.

Kuhn, J., 2005, "Effect of Cracking on the Hydraulic Properties of Unsaturated Highly Plastic Clays." MS thesis, The University of Texas, Texas.

Lee, J., and Fox, P., 2005, "Efficiency of Seepage Consolidation for Preparation of Clay Substrate for Centrifuge testing." *Geotechnical Testing Journal*, Vol. 28, No. 6, pp.1–9.

Lu, N., and Likos, W.J, 2005, *Unsaturated Soil Mechanics*, Wiley, New York.

Lytton, R. L., Aubeny, C., and Bulut, R., May 2006, "Design Procedure for Pavements on Expansive Soils: Volume 2," Texas Transportation Institute, Report # 0-4518-1 (V2).

Lytton, R. L., Aubeny, C., and Bulut, R., August 2005, "Design Procedure for Pavements on Expansive Soils: Volume 1," Texas Transportation Institute, Report # 0-4518-1 (V1).

Lytton, R. L., Aubeny, C., and Bulut, R., June 2005, "Design Procedure for Pavements on Expansive Soils: Volume 3," Texas Transportation Institute, Report # 0-4518-1 (V3).

Lytton, R. L., Aubeny, C., and Bulut, R., July 2005, "Re-evaluation of Potential Vertical Rise Design Procedures 0-4518-S," Texas Transportation Institute, Report # 0-4518-S.

McCartney, J., 2006, "Measurement of the Hydraulic Characteristics of Unsaturated Soils using a Centrifuge Permeameter," Comprehensive Proposal, The University of Texas at Austin.

McCartney, J. S., and Zornberg, J. G. (2005). "The Centrifuge Permeameter for Unsaturated Soils (CPUS)." Proceedings of the International Symposium on Advanced Experimental

Unsaturated Soil Mechanics, Experus 2005, Trento, Italy, June 27-29, A.A. Balkema, pp.299–304.

McDowell, C., 1956, "Interrelationships of loads, volume change, and layer thickness of soils to the behavior of engineering structures." Highway Research Board, Proc. 35th Annual Meetings, Pub. No. 426, Washington, DC, pp. 754–772.

Olson, Roy E. 2007 Course Notes on Incremental Vertical-Flow Consolidation Test, Consolidation and Settlement of Soft Soils.

Mitchell, R. J., 1994, "Centrifuge techniques for testing clay liner samples." *Canadian Geotechnical Journal*, No. 31, pp. 577–583.

Puppala, A., and Hoyos, L., Ongoing, "Realistic design guidelines for low classification roads in high PI clays." Texas Department of Transportation Project #0-5430.

Robinson, R. G., Tan, T. S., and Lee, F. H., 2003, "A Comparative Study of Suction-Induced Seepage Consolidation Versus Centrifuge Consolidation." *Journal of Geotechnical Testing*, March 2003, Vol. 26, No.1., pp 1–10.

Singh, D., and Gupta, A., 2000, "Modeling hydraulic conductivity in a small centrifuge." *Canadian Geotechnical Journal*, No. 37, pp. 1150–1155.

Terzaghi, K., 1943, *Theoretical Soil Mechanics.* John Wiley and Sons, New York.

Weisberg, E., and Frydman, S., 1990, "Study of Flow in Compacted Columns of Swelling Clay."

Zornberg, J. G. and Kuhn, J., 2007, Field Suction and Effect of Cracking in Highly Plastic Clay, Center for Transportation Research, Report # 0-5202-1 through # 0-5202-3.

Appendix A: Small Centrifuge Testing Procedure

Appendix A presents 5-6048-01-P2, *Swelling of Highly Plastic Clays under Centrifuge Loading*, a document detailing the small centrifuge testing procedure.

A.1 Soil Preparation

In order to prepare the soil for centrifuge testing, the processed soil was passed through Sieve #10 into a mixing bowl, until approximately 300 grams of sieved soil was obtained. The appropriate amount of distilled water was added using a spray bottle to achieve the target water content. Usually, 3.5% additional water mass was added to the soil to account for water loss during the mixing process. A light coat of water was sprayed on the surface of the soil and mixed into the soil using a spatula. This was repeated until the water within the spray bottle was depleted. The soil and water were also hand mixed in addition to mixing with the spatula. The soil and water mixture was placed in a Ziploc bag for at least one day. This allowed the water to evenly distribute throughout the soil particles. The acceptable range of water contents for centrifuge testing was approximately +/- 0.5% of the target water content.

A.2 Permeameter Cup Preparation

The top cup, cup base, and the porous disks were cleaned and air dried before each centrifuge test. These components are shown in Figure 1.

Figure 1: Components of Plastic Permeameter Cup: Top Cup, Cup Base, and Porous Disks

The top and base were shaken vigorously to remove any water in the small crevices, and the porous disks were shaken on a paper towel in order to remove water trapped within the 1/32” holes. The following list describes the permeameter cup preparation after it has been cleaned and dried:

- Overlay the porous disk with the filter paper, and use scissors to cut the filter paper to the diameter of the disk. Two filter papers are required for each permeameter cup.
- Record the mass of the top cup and cup base and screw the base to the top cup.
- Insert a porous disk to rest on the bottom ledge of the top cup.

- Place a thin layer of vacuum grease 1.5 cm high on the inside rim of the bottom of the top cup. This is the area where the compacted and expanding soil will be in contact with the cup.
- Insert the cut filter paper on top of the porous disk and press down to ensure the filter paper, porous disk, and cup ledge are in good contact with one another.
- Record the mass of the constructed cup.
- Record the height of the cup to the nearest 1/1000” using the mounted caliper. The caliper arm is placed inside the opening of the top cup until the tip of the arm contacts the small metallic plate that is on top of the filter paper. Adjust the position of the cup to where the height measurement can be taken in the center of the filter paper. To determine the target height of the compacted soil specimen within the permeameter cup, 1 cm is added to this height (1 cm corresponds to the target sample height after compaction).
- Using the mounted caliper, record the height of the top porous disk lying on top of the filter paper.

A.3 Soil Sample Compaction

The test specimens were compacted to a height of 1 cm. In order to obtain a 1 cm high specimen compacted to the desired dry unit weight, the mass of soil required to achieve the testing conditions was predetermined. Knowing the target dry unit weight, the target water content, and specimen height and diameter, we then back-calculated the mass of soil needed to achieve the desired conditions.

The specimen height was monitored throughout the compaction process using a small metal plate with a thickness of 0.039” as shown in Figure 2. The marks on the metal plate designate the point at which the caliper arm is placed to measure the specimen height. The specimen height is monitored on five points across the surface of the specimen: the middle, top, right, bottom, and left as shown in Figure 2. The air vent along the top cup serves as the reference point for taking the different height measurements across the specimen’s surface.

(a) ***(b)***

Figure 2: (a) Location of Sample Height Measurements throughout Testing Procedure
(b) Metal Plate Used in Determining Sample Height

The subsequent stages in the test procedure are as follows:

- Place the constructed permeameter cup on the scale and zero it. Pour the predetermined mass of cured soil out of the Ziploc bag into the cup using a funnel. During the pouring process, it is beneficial to pause and vibrate the cup by shaking and/or tapping to evenly distribute the soil particles. To account for soil mass loss during compaction, we recommend adding 0.1 grams of soil to the predetermined mass. Once all of the soil has been poured into the cup, check to see if the soil has been distributed evenly. Sometimes, manual adjustment of the soil particles may be needed to prevent significant unequal densities within the soil.
- Close the Ziploc bag to keep the cured soil from losing moisture. The water content of this soil will be taken later in the test procedure.
- Begin compacting using your thumb in order to densify the soil enough to withstand the bearing load produced by the small diameter compactor (Figure 3).

Figure 3: Densification of Soil Using Thumb

- Begin to compact the soil using the small diameter kneading compactor (Figure 4), while trying to maintain a constant height across the top surface of the specimen. Continue to monitor the change in specimen height using the vertical caliper and the metal plate.
    - Note: the small diameter kneading compactor creates an uneven surface on the top of the compacted specimen. In order to create a flatter surface for the top filter paper and porous disk to sit on, we used the larger diameter compactor in conjunction with a rubber mallet, as described in the next bullet point.

Figure 4: Compaction of Soil Specimen Using Small Diameter Kneading Compactor

- When the specimen height reaches approximately 0.03” from the target height, begin compacting the soil with the large diameter compactor. Slide the compaction rod along the inner wall of the permeameter cup until it is sitting on the soil specimen; hold the compactor in place with your thumb. The bottom of the compactor should be flush with the soil, and the side of the compactor should be flush with the inner wall of the cup. Using the side of the rubber mallet, gently tap the top of the compactor four times (Figure 5). Rotate the cup 45 degrees, and continue the tapping procedure until the full 360 degree rotation is completed. Check the specimen height at the locations previously mentioned after each 360 degree rotation.
    - Note: soil will rise along the inner diameter of the top cup due to compaction. Remove the soil by using a dental hook along the rim of the top of the specimen. This soil should be placed back in the cup and re-compacted using the small kneading compactor prior to continuing with the large diameter compactor.

Figure 5: Compaction of Soil Specimen Using Rubber Mallet and Large Diameter Compaction Rod

- Alternate between the compaction techniques (using the small and large compactors) until the target height is reached. During this point in the compaction process, the small compactor is most useful in densifying a small area of the specimen in order to achieve the 1 cm specimen height in that location.
- Record the final specimen heights using the metal plate at the middle, top, right, bottom, and left of the sample (Figure 6).
    - Note: it is critical that the soil specimen is compacted as close to 1 cm as possible in the center, since this is where the in-flight data acquisition system will be recording the swell data. An acceptable range for the middle sample height was deemed +0.001” and -0.002” from the target height. Regarding the top, right, bottom, and left sample heights, an acceptable range was +0.002” and -0.005” from the target height.

Figure 6: Measurement of Compacted Specimen Using Metal Plate and Mounted Caliper

- Record the mass of the permeameter cup and the compacted soil.

A.4 Permeameter Cup Assembly

The procedure for assembling the permeameter cup after the sample has been compacted within the tolerable range involved the following:

- Place the filter paper and the top porous disk on the soil and seat it with your thumb by applying pressure in the center of the porous disk.
- Record the height of the sample at the center of the cup using the mounted caliper
- Record the mass of the permeameter cup.
- Record the mass of the overburden washers and place them upon the top porous disk.
- Place approximately 25.65 grams of stacked washers on the top porous disk. Make sure the center of the washers aligns with the center of the porous disk (Figure 7). The 26.65 grams simulate half the weight of the 2 cm of water head to be added during the swelling process.

Figure 7: Assembled Permeameter Cup with Overburden Washers and Washers Simulating 51.3 Grams of Overburden from the Ponded Water

- Insert the assembled permeameter cup into the metal swing-out bucket. The metal buckets should already be hanging from the arms of the rotor within the centrifuge.
- Insert the linear position sensor (LPS) into the center holes of the washers until it reaches the center of the top porous disk. Ensure there is good contact between the LPS and the top porous disk, as well as good contact between the top cap and the permeameter cup.
- Place a piece of electrical tap along the metal bucket and top cap in order to stabilize the LPS during centrifugation.
- Adjust the centrifuge RPMs to the desired testing conditions.
- The final assembly is displayed in Figure 8.

Figure 8: Assembled Testing Setup within the Centrifuge

A.5 Seating Load and Compression Cycles

The seating load and compression cycles of the specimen determine the seating height of the sample and the height of the specimen after compaction. Two cycles are completed to ensure these heights have been accurately measured by the data acquisition system. Following are the steps to complete the compression/decompression cycles:

- Press the START button on the control board of the centrifuge.
- Monitor the accelerometer readings to determine when the g-Level reaches a value corresponding to 2–3 g's. After reaching the target g-Level, wait approximately 5 minutes or however long it takes for the height measurements to reach a constant level.
- Adjust the RPM dial reading accordingly to obtain the target g-Level for the test. After reaching the target g-Level, wait at least 15 minutes for the height of the samples to reach a constant level.
- Press STOP on the centrifuge and wait until the accelerometer reading signifies the centrifuge is no longer spinning.

A.6 Final Permeameter Cup Preparation

- Remove the permeameter cup from the metal bucket and take out the metal washers from inside the cup.
- Insert the washers, providing the overburden mass for the permeameter cup.
- Zero the mass of the cup on the scale and add 51.3 grams of distilled water to the cup (51.3 grams of water is the mass that approximately corresponds to 2 cm of ponded water head) (Figure 9).

Figure 9: Final Permeameter Cup Assembly with 2 cm of Ponded Water Head and Overburden Washer

- Insert the cup into the centrifuge as described in Section A.4.
- Wait for one output reading and then press START. Monitor the accelerometer reading to ensure the centrifuge reaches the target g-Level and adjust the RPMs if needed.
- Take the water content of the mixed soil in the Ziploc bag according to ASTM D 2216. This water content is the compaction water content for the test specimen.

A.7 Test Duration

The protocol used in this study involves running the centrifuge test for 2 days. The 2-day test duration was chosen for the following reasons:

1. Primary swelling of the sample is completed within 1 day of starting the centrifuge test.
2. Secondary swell is observed and its rate can be determined when the swell data is plotted on a semi-log scale.
3. Little information is gained regarding the swell potential and behavior of soils when the test continues for longer than 2 days.

A.8 Test Termination

After the 2-day centrifuge testing period, the test is terminated with the following procedure:

- Push STOP on the centrifuge and flip the switch activating the max brake. Wait for the centrifuge to stop spinning.
- Once the centrifuge has stopped spinning, and one more output reading has taken place, press the stop button on the Labview program control screen.
- Push STOP again to deactivate the magnetic locking mechanism for the centrifuge door. Open it and remove the permeameter cups from the metal buckets.
- Record the weight of the permeameter cup.
- Record the weight of the base of the permeameter cup and pour out the outflow water.
- Remove the overburden washer and pour out the ponded water. We recommend applying pressure with the thumb to the center of the top porous disk during the pouring process. This helps ensure that most of the water trapped between the interfaces of the porous disk, filter paper, and the specimen is removed, and not incorporated into the hand-measurement of the swell potential.
- Attach the cup base to the top cup and record the heights of the specimens in the previously described locations (Figure 2).
- Remove the soil specimen by unscrewing the cup base and sliding the specimen from the bottom to the top of the cup.
- Gently dry the outer surface of the test specimen and take a water content measurement according to ASTM D 2216.
    - Note: the soil sample will have small pockets of water on its top surface due to the ponded water added for the centrifuge swell testing. These water pockets are not absorbed by the soil, and should not be considered in final water content measurement after swelling has taken place. Therefore, the water is removed by gently patting the outer specimen surface with a paper towel.

Appendix B: Centrifuge Testing Summary Sheet

Key for TxDOT Summary Sheet of Centrifuge Testing

Column A	Sample Number	The number of the compacted sample run
Column B	Test Date	The date the test was run
Column C	Test ID Number	The ID Number consists of the following: Type of Clay – Target G-Level – Target Moisture Content – Target Relative Compaction – Cup Number
Column D	Cup Number	The number of the cup the soil was in
Column E	Test Operator	The person who ran the test
Column F	Soil Type	The soil that was run. EF is Eagle Ford, BT is Black Taylor, and HB is Houston Black.
Column G	Target G-Level	The G-Level that was aimed for during the test
Column H	Actual G-Level	The average G-Level during the test. Note: Does not include the compression and decompression cycle.
Column I	Water Content	The target water content condition. OPT is Optimum, WOPT is Wet of Optimum, and DOPT is Dry of Optimum.
Column J	Target Water Content (%)	The desired water content of the soil during compaction
Column K	Actual Water Content (%)	The actual water content of the soil during compaction
Column L	Relative Compaction (%)	The target relative compaction for the test. $RC = \gamma_{d,actual}/\gamma_{d,max}$
Column M	Target Dry Unit Weight (kN/m^3)	The target dry unit weight following compaction that would give the desired RC
Column N	Actual Dry Unit Weight (kN/m^3)	The actual dry unit weight of soil following compaction
Column O	Sample Height (cm)	The height of the soil sample after compaction
Column P	Overburden Mass (g)	The mass of overburden on the soil during testing. This value includes the weight of the washers and LPS, but not the weight of the water.
Column Q	Height of Water (cm)	The height of the water added to the soil before placement in the centrifuge
Column R	End of Swell Water Content (%)	The water content of the soil after the test had been run and soil had swelled

Column S	Change in Water Content (%)	The difference in the water content between the soil at compaction and soil at the end of the test
Column T	Swell (%)	The vertical swell of the soil during the test

Note: For basic characterization properties (i.e., Plasticity Index, Soil Classification, Sieve Analysis, Optimum Moisture Content, and Maximum Dry Density as determined by the Standard Proctor Test), see Section 2.2 of the main report.

Sample #	Test Date	Test ID Number	Cup #	Test Operator	Soil Type	Target G-Level	Actual G-Level	Water Content	Target Water Content (%)	Actual Water Content (%)	Mass added (g)	Dry Unit Weight	Target Dry Unit Weight (kN/m3)	Actual Dry Unit Weight (kN/m3)	Sample Height (cm)	*Overburden Mass (g)	Height of Water (cm)	End of Swell Water Content (%)	Change in Water Content (%)	Swell (%)
1	10-14-11	EF-25-OPT-100-1	1	Trevor	EF	25	23.9	OPT	24	24.43	49.96	100	15.25	15.22	1.000	21.09	2	40.87	16.44	18.87
2	10-14-11	EF-25-OPT-100-2	2	Trevor	EF	25	23.9	OPT	24	24.43	49.91	100	15.25	15.17	1.003	21.14	2	40.60	16.17	18.42
3	10-18-11	EF-200-OPT-100-1	1	Trevor	EF	200	195.7	OPT	24	24.40	50.05	100	15.25	15.25	1.000	21.08	2	34.67	10.27	8.99
4	10-18-11	EF-200-OPT-100-2	2	Trevor	EF	200	195.7	OPT	24	24.40	49.94	100	15.25	15.22	1.000	21.21	2	34.77	10.37	8.58
5	10-22-11	BT-25-OPT-100-1	1	Trevor	BT	25	28.9	OPT	23.3	23.67	49.89	100	15.34	15.33	0.997	21.08	2	27.59	3.92	2.63
6	10-22-11	BT-25-OPT-100-2	2	Trevor	BT	25	28.9	OPT	23.3	23.67	49.95	100	15.34	15.35	0.997	21.21	2	27.35	3.68	2.03
7	10-25-11	BT-200-OPT-100-1	1	Trevor	BT	200	203.1	OPT	23.3	23.57	50.01	100	15.34	15.34	1.000	21.08	2	26.12	2.55	1.55
8	10-25-11	BT-200-OPT-100-2	2	Trevor	BT	200	203.1	OPT	23.3	23.57	49.91	100	15.34	15.31	1.000	21.22	2	26.12	2.55	1.67
9	11-1-11	S5-5-OPT-100-1	1	Trevor	S5	5	5.0	OPT	12.6	12.60	-	100	18.92	18.90	1.000	22.26	2	-	-	0.60
10	11-1-11	S5-20-OPT-100-1	1	Trevor	S5	25	25.0	OPT	12.6	12.60	-	100	18.92	18.90	1.000	22.26	2	-	-	0.60
11	11-1-11	S5-200-OPT-100-1	1	Trevor	S5	200	200.0	OPT	12.6	12.60	-	100	18.92	18.90	1.000	22.26	2	-	-	0.60
12	11-1-11	S5-20-OPT-100-2	2	Trevor	S5	25	25.0	OPT	12.6	12.60	-	100	18.92	18.90	1.000	22.26	2	-	-	0.60
13	11-4-11	HB-25-OPT-100-1	1	Trevor	HB	25	30.2	OPT	25.5	25.47	48.79	100	14.72	14.74	1.000	21.09	2	29.70	4.23	2.28
14	11-4-11	HB-25-OPT-100-2	2	Trevor	HB	25	30.2	OPT	25.5	25.47	48.63	100	14.72	14.69	1.000	21.21	2	30.27	4.80	3.18
15	12-20-11	EF-25-OPT-97-1	1	Trevor	EF	25	27.4	OPT	24	23.86	48.51	97	14.79	14.96	0.992	21.22	2	42.12	18.26	17.76
16	12-20-11	EF-25-WOPT-97-2	2	Trevor	EF	25	27.4	WOPT	27	27.36	49.62	97	14.79	14.77	1.000	21.08	2	43.58	16.22	13.99
17	12-20-11	EF-25-WOPT-97-3	3	Trevor	EF	25	27.4	WOPT	27	27.36	49.48	97	14.79	14.76	0.997	21.07	2	42.96	15.60	12.99
18	12-20-11	EF-25-OPT-97-4	4	Trevor	EF	25	27.4	OPT	24	23.86	48.40	97	14.79	14.85	0.997	21.21	2	44.32	20.46	17.51
19	1-11-12	EF-25-OPT-94-1	1	Trevor	EF	25	25.2	OPT	24	23.57	46.91	94	14.34	14.50	0.992	21.21	2	42.94	19.37	17.57
20	1-11-12	HB-25-OPT-97-2	2	Trevor	HB	25	25.2	OPT	25.5	25.34	47.42	97	14.28	14.34	1.000	21.08	2	32.12	6.78	4.75
21	1-11-12	HB-25-OPT-97-3	3	Trevor	HB	25	25.2	OPT	25.5	25.34	47.39	97	14.28	14.33	1.000	21.07	2	32.02	6.68	5.93
22	1-11-12	EF-25-OPT-94-4	4	Trevor	EF	25	25.2	OPT	24	23.57	46.90	94	14.34	14.39	1.000	21.21	2	43.10	19.53	18.07
23	1-13-12	EF-200-OPT-94-1	1	Trevor	EF	200	200.2	OPT	24	24.04	46.88	94	14.34	14.36	0.997	21.06	2	37.60	13.56	7.57
24	1-13-12	EF-200-OPT-94-4	4	Trevor	EF	200	200.2	OPT	24	24.04	46.88	94	14.34	14.33	1.000	21.07	2	37.56	13.52	7.08
25	1-20-12	HB-25-OPT-100-1	1	Trevor	HB	25	26.6	OPT	25.5	25.13	48.59	100	14.72	14.72	1.000	21.07	2	30.31	5.18	3.15
26	1-20-12	HB-25-OPT-94-2	2	Trevor	HB	25	26.6	OPT	25.5	25.13	45.85	94	13.84	13.89	1.000	21.24	2	35.16	10.03	4.91
27	1-20-12	HB-25-OPT-94-3	3	Trevor	HB	25	26.6	OPT	25.5	25.13	46.20	94	13.84	13.96	1.003	21.2	2	34.32	9.19	4.55
28	1-20-12	HB-25-OPT-100-4	4	Trevor	HB	25	26.6	OPT	25.5	25.13	48.51	100	14.72	14.77	0.995	21.07	2	31.33	6.20	4.65
29	1-24-12	HB-200-OPT-100-1	1	Trevor	HB	200	203.1	OPT	25.5	25.07	48.87	100	14.72	14.81	1.000	21.07	2	29.58	4.51	2.65
30	1-24-12	HB-200-OPT-94-2	2	Trevor	HB	200	203.1	OPT	25.5	25.07	45.83	94	13.84	13.89	1.000	21.24	2	32.08	7.01	2.85
31	1-24-12	HB-200-OPT-94-3	3	Trevor	HB	200	203.1	OPT	25.5	25.07	45.86	94	13.84	13.90	1.000	21.21	2	32.15	7.08	3.11
32	1-24-12	HB-200-OPT-100-4	4	Trevor	HB	200	203.1	OPT	25.5	25.07	48.80	100	14.72	14.79	1.000	21.07	2	30.02	4.95	2.84
33	1-26-12	BT-25-OPT-97-1	1	Trevor	BT	25	26.2	OPT	23.3	23.63	48.47	97	14.88	14.86	1.000	21.24	2	29.66	6.03	3.34
34	1-26-12	BT-25-WOPT-97-2	2	Trevor	BT	25	26.2	WOPT	26.3	26.65	49.62	97	14.88	14.85	1.000	21.07	2	29.71	3.06	2.42
35	1-26-12	BT-25-WOPT-97-3	3	Trevor	BT	25	26.2	WOPT	26.3	26.65	49.74	97	14.88	14.85	1.003	21.08	2	29.21	2.56	1.66
36	1-26-12	BT-25-OPT-97-4	4	Trevor	BT	25	26.2	OPT	23.3	23.63	48.43	97	14.88	14.85	1.000	21.21	2	29.83	6.20	3.30
37	1-28-12	BT-200-OPT-97-1	1	Trevor	BT	200	202.6	OPT	23.3	23.10	48.42	97	14.88	14.91	1.000	21.24	2	30.07	6.97	2.64
38	1-28-12	BT-200-WOPT-97-2	2	Trevor	BT	200	202.6	WOPT	26.3	26.19	49.67	97	14.88	14.92	1.000	21.07	2	27.59	1.40	1.28
39	1-28-12	BT-200-WOPT-97-3	3	Trevor	BT	200	202.6	WOPT	26.3	26.19	49.70	97	14.88	14.93	1.000	21.07	2	24.46	-1.73	0.93
40	1-28-12	BT-200-OPT-97-4	4	Trevor	BT	200	202.6	OPT	23.3	23.10	48.43	97	14.88	14.95	0.997	21.2	2	26.95	3.85	1.88
41	1-31-12	BT-25-OPT-100-1	1	Trevor	BT	25	27.1	OPT	23.3	23.52	49.96	100	15.34	15.37	0.997	21.24	2	28.22	4.70	3.90
42	1-31-12	BT-25-OPT-94-2	2	Trevor	BT	25	27.1	OPT	23.3	23.52	46.89	94	14.42	14.50	0.992	21.07	2	30.60	7.08	3.25
43	1-31-12	BT-25-OPT-94-3	3	Trevor	BT	25	27.1	OPT	23.3	23.52	46.94	94	14.42	14.44	0.997	21.07	2	29.92	6.40	2.21
44	1-31-12	BT-25-OPT-100-4	4	Trevor	BT	25	27.1	OPT	23.3	23.52	49.99	100	15.34	15.34	1.000	21.2	2	27.77	4.25	3.64
45	2-2-12	BT-200-OPT-100-1	1	Trevor	BT	200	201.8	OPT	23.3	23.82	49.92	100	15.34	15.32	0.997	21.24	2	27.17	3.35	1.98
46	2-2-12	BT-200-OPT-100-4	4	Trevor	BT	200	201.8	OPT	23.3	23.82	49.88	100	15.34	15.27	1.000	21.2	2	26.90	3.08	1.84
47	2-4-12	EF-25-OPT-97-2	2	Trevor	EF	25	25.7	OPT	24	24.37	48.46	97	14.79	14.77	1.000	21.07	2	41.52	17.15	17.14
48	2-4-12	EF-25-OPT-97-3	3	Trevor	EF	25	25.7	OPT	24	24.37	48.37	97	14.79	14.74	1.000	21.07	2	41.11	16.74	16.04
49	2-6-12	BT-200-DOPT-97-1	1	Trevor	BT	200	201.9	DOPT	20.3	20.35	47.22	97	14.88	14.91	0.997	21.24	2	29.44	9.09	4.96
50	2-6-12	EF-200-OPT-97-2	2	Trevor	EF	200	201.9	OPT	24	23.61	48.40	97	14.79	14.92	0.995	21.07	2	35.75	12.14	8.52
51	2-6-12	EF-200-OPT-97-3	3	Trevor	EF	200	201.9	OPT	24	23.61	48.34	97	14.79	14.82	1.000	21.07	2	35.97	12.36	8.14
52	2-6-12	BT-200-DOPT-97-4	4	Trevor	BT	200	201.9	DOPT	20.3	20.35	47.34	97	14.88	14.91	1.000	21.2	2	29.76	9.41	5.25
53	2-8-12	EF-200-WOPT-97-1	1	Trevor	EF	200	199.4	WOPT	27	27.30	49.49	97	14.79	14.77	0.997	21.23	2	35.93	8.63	5.61
54	2-8-12	EF-200-DOPT-97-2	2	Trevor	EF	200	199.4	DOPT	21	21.28	47.17	97	14.79	14.74	1.000	21.05	2	37.17	15.89	7.77
55	2-8-12	EF-200-DOPT-97-3	3	Trevor	EF	200	199.4	DOPT	21	21.28	47.30	97	14.79	14.78	1.000	21.07	2	37.82	16.54	7.90
56	2-8-12	EF-200-WOPT-97-4	4	Trevor	EF	200	199.4	WOPT	27	27.30	49.44	97	14.79	14.80	0.995	21.2	2	35.68	8.38	5.95
57	2-10-12	BT-25-DOPT-97-1	1	Trevor	BT	25	25.4	DOPT	20.3	20.79	47.27	97	14.88	14.87	0.997	21.23	2	30.93	10.14	5.87
58	2-10-12	EF-25-DOPT-97-2	2	Trevor	EF	25	25.4	DOPT	21	21.45	47.24	97	14.79	14.82	0.995	21.07	2	42.56	21.11	18.71
59	2-10-12	EF-25-DOPT-97-3	3	Trevor	EF	25	25.4	DOPT	21	21.45	47.21	97	14.79	14.77	0.997	21.07	2	42.97	21.52	18.35

60	2-10-12	BT-25-DOPT-97-4	4	Trevor	BT	25	25.4	DOPT	20.3	20.79	47.24	97	14.88	14.90	0.995	21.2	2	31.30	10.51	7.13
61	2-13-12	HB-5-OPT-97-2	2	Trevor	HB	5	7.1	OPT	25.5	25.11	47.30	97	14.28	14.33	1.000	21.07	2	33.45	8.34	5.76
62	2-13-12	HB-5-OPT-97-3	3	Trevor	HB	5	7.1	OPT	25.5	25.11	47.29	97	14.28	14.29	1.003	21.07	2	31.44	6.33	6.50
63	2-15-12	HB-25-OPT-100-1	1	Trevor	HB	25	27.0	OPT	25.5	25.83	48.77	100	14.72	14.73	0.997	21.23	2	30.91	5.08	4.63
64	2-15-12	HB-25-OPT-100-2	2	Trevor	HB	25	27.0	OPT	25.5	25.83	48.69	100	14.72	14.63	1.003	21.2	2	29.54	3.71	3.17
65	2-17-12	BT-5-OPT-97-1	1	Trevor	BT	5	6.7	OPT	23.3	23.27	48.36	97	14.88	14.87	1.000	21.17	2	30.81	7.54	4.66
66	2-17-12	BT-5-OPT-97-4	4	Trevor	BT	5	6.7	OPT	23.3	23.27	48.39	97	14.88	14.88	1.000	21.21	2	29.87	6.60	7.11
67	2-17-12	EF-5-OPT-100-2	2	Trevor	EF	5	6.7	OPT	24	23.91	49.84	100	15.25	15.29	0.997	21.06	2	47.25	23.34	29.81
68	2-17-12	EF-5-OPT-100-3	3	Trevor	EF	5	6.7	OPT	24	23.91	49.98	100	15.25	15.25	1.003	21.07	2	48.31	24.40	31.12
69	2-21-12	HB-200-WOPT-97-1	1	Trevor	HB	200	202.2	WOPT	28.5	28.41	48.24	97	14.28	14.24	1.000	21.06	2	30.47	2.06	1.37
70	2-21-12	HB-200-DOPT-97-2	2	Trevor	HB	200	202.2	DOPT	22.5	22.61	46.37	97	14.28	14.30	1.003	21.17	2	30.04	7.43	2.21
71	2-21-12	HB-200-DOPT-97-3	3	Trevor	HB	200	202.2	DOPT	22.5	22.61	46.13	97	14.28	14.26	1.000	21.2	2	29.96	7.35	2.17
72	2-21-12	HB-200-WOPT-97-4	4	Trevor	HB	200	202.2	WOPT	28.5	28.41	48.55	97	14.28	14.33	1.000	21.07	2	30.70	2.29	1.48
73	3-6-12	HB-25-WOPT-97-1	1	Trevor	HB	25	26.2	WOPT	28.5	28.00	48.46	97	14.28	14.35	1.000	21.17	2	30.90	2.90	2.01
74	3-6-12	HB-25-DOPT-97-2	2	Trevor	HB	25	26.2	DOPT	22.5	22.15	46.22	97	14.28	14.49	0.990	21.05	2	33.34	11.19	6.57
75	3-6-12	HB-25-DOPT-97-3	3	Trevor	HB	25	26.2	DOPT	22.5	22.15	46.15	97	14.28	14.32	1.000	21.06	2	33.34	11.19	6.07
76	3-6-12	HB-25-WOPT-97-4	4	Trevor	HB	25	26.2	WOPT	28.5	28.00	48.35	97	14.28	14.39	0.995	21.21	2	30.85	2.85	1.59
77	3-8-12	HB-200-OPT-97-2	2	Trevor	HB	200	199.5	OPT	25.5	25.97	47.34	97	14.28	14.28	0.997	21.05	2	29.74	3.77	1.58
78	3-8-12	HB-200-OPT-97-3	3	Trevor	HB	200	199.5	OPT	25.5	25.97	47.29	97	14.28	14.23	1.000	21.05	2	29.18	3.21	1.34
79	3-12-12	EF-200-DOPT-97-1	1	Trevor	EF	200	200.8	DOPT	21	21.44	47.15	97	14.79	14.72	1.000	21.16	2	35.88	14.44	7.52
80	3-12-12	EF-200-DOPT-97-4	4	Trevor	EF	200	200.8	DOPT	21	21.44	47.19	97	14.79	14.81	0.995	21.2	2	35.78	14.34	7.82
81	3-17-12	EF-200-OPT-97-1	1	Trevor	EF	200	200.7	OPT	24	24.35	48.27	97	14.79	14.75	0.997	21.17	2	33.72	9.37	6.21
82	3-17-12	EF-200-OPT-97-4	4	Trevor	EF	200	200.7	OPT	24	24.35	48.27	97	14.79	14.79	0.995	21.2	2	33.99	9.64	6.17
83	3-19-12	EF-100-OPT-97-1	1	Trevor	EF	100	100.2	OPT	24	24.28	48.43	97	14.79	14.77	1.000	21.16	2	35.77	11.49	9.63
84	3-19-12	EF-100-OPT-97-4	4	Trevor	EF	100	100.2	OPT	24	24.28	48.27	97	14.79	14.76	0.997	21.2	2	35.50	11.22	8.98
85	3-23-12	EF-5-OPT-97-1	1	Trevor	EF	5	6.7	OPT	24	24.08	48.32	97	14.79	14.80	0.997	21.15	2	48.59	24.51	27.31
86	3-23-12	EF-5-OPT-97-4	4	Trevor	EF	5	6.7	OPT	24	24.08	48.32	97	14.79	14.76	1.000	21.21	2	47.30	20.08	26.68
87	3-28-12	BT-25-OPT-94-1	1	Trevor	BT	25	27.4	OPT	23.3	23.16	46.91	94	14.42	14.51	0.995	21.15	2	29.79	6.63	3.12
88	3-28-12	BT-25-OPT-94-4	4	Trevor	BT	25	27.4	OPT	23.3	23.16	46.85	94	14.42	14.42	1.000	21.21	2	29.44	6.28	3.18
89	4-5-12	BT-200-OPT-94-1	1	Trevor	BT	200	200.7	OPT	23.3	23.25	46.87	94	14.42	14.45	0.997	21.14	2	27.95	4.70	1.25
90	4-5-12	BT-200-OPT-94-4	4	Trevor	BT	200	200.7	OPT	23.3	23.25	46.93	94	14.42	14.47	0.997	21.2	2	29.54	6.29	2.98
91	4-12-12	EF-25-OPT-97-1	1	Trevor	EF	25	26.6	OPT	24	24.03	48.33	97	14.79	14.77	1.000	21.14	2	44.65	20.62	15.30
92	4-12-12	EF-25-OPT-97-4	4	Trevor	EF	25	26.6	OPT	24	24.03	48.46	97	14.79	14.81	1.000	21.2	2	44.37	20.34	15.33
93	7-9-12	EF-5-OPT-97-2	2	Das	EF	5	4.8	OPT	24	24.20	48.59	97	14.79	14.86	0.998	22.26	2.00	47.06	22.86	19.41
94	7-14-12	EF-5-OPT-97-1	1	Das	EF	5	5.7	OPT	24	24.40	48.61	97	14.79	14.84	0.998	22.26	2.00	48.24	23.84	20.39
95	7-14-12	EF-5-OPT-97-2	2	Das	EF	5	5.7	OPT	24	24.40	48.61	97	14.79	14.84	0.998	22.27	2.00	48.61	24.21	20.94
96	7-14-12	EF-5-OPT-100-3	3	Das	EF	5	5.7	OPT	24	24.40	49.61	100	15.25	15.13	0.999	21.62	2.00	48.05	23.65	21.35
97	7-14-12	EF-5-OPT-100-4	4	Das	EF	5	5.7	OPT	24	24.40	49.61	100	15.25	15.13	0.999	21.72	2.00	48.34	23.94	22.59
98	7-19-12	BT-5-OPT-97-1	1	Das	BT	5	6.0	OPT	23.3	23.70	48.79	97	14.88	14.95	1.000	22.26	2.00	26.95	3.25	1.52
99	7-19-12	BT-5-OPT-97-2	2	Das	BT	5	6.0	OPT	23.3	23.70	48.27	97	14.88	14.79	1.000	22.26	2.00	5.73	4.09	1.64
100	8-5-12	EF-5-OPT-94-1	1	Das	EF	5	7.3	OPT	24	23.80	46.74	94	14.34	14.31	1.000	22.26	2.00	44.46	20.66	19.00
101	8-5-12	BT-5-OPT-94-2	2	Das	BT	5	7.3	OPT	23.3	23.70	46.86	94	14.42	14.36	1.000	22.27	2.00	29.08	5.38	2.37
102	8-11-12	EF-25-OPT-97-1	1	Das	EF	25	26.6	OPT	24	24.30	48.01	97	14.79	14.64	1.000	22.26	2.00	36.76	12.46	10.37
103	8-11-12	EF-25-OPT-97-2	2	Das	EF	25	26.6	OPT	24	24.30	48.17	97	14.79	14.69	1.000	22.27	2.00	38.52	14.22	11.21
104	8-11-12	BT-25-OPT-97-3	3	Das	BT	25	26.6	OPT	23.3	23.80	48.37	97	14.88	14.81	1.000	21.62	2.00	28.04	4.24	1.32
105	9-19-12	BT-5-OPT-94-1	1	Das	BT	5	7.3	OPT	23.3	23.80	46.87	94	14.42	14.35	1.000	22.26	2.00	29.88	6.08	1.72
106	9-19-12	BT-5-OPT-94-2	2	Das	BT	5	7.3	OPT	23.3	23.80	46.74	94	14.42	14.34	0.998	22.27	2.00	30.09	6.29	1.81
107	9-19-12	BT-5-OPT-100-4	4	Das	BT	5	7.3	OPT	23.3	23.80	49.84	100	15.34	15.26	1.000	21.72	2.00	31.96	8.16	2.04
108	9-26-12	BT-5-DOPT-97-1	1	Das	BT	5	7.6	DOPT	20.3	20.60	47.47	97	14.88	14.92	1.000	22.26	2.00	29.56	8.96	4.47
109	9-26-12	BT-5-DOPT-97-2	2	Das	BT	5	7.6	DOPT	20.3	20.60	47.53	97	14.88	14.94	1.000	22.26	2.00	29.62	9.02	4.76
110	9-26-12	BT-5-WOPT-97-4	4	Das	BT	5	7.6	WOPT	26.3	25.90	49.57	97	14.89	14.97	0.997	21.72	2.00	28.21	2.31	1.49
111	10-1-12	HB-5-DOPT-97-1	1	Das	HB	5	7.8	DOPT	22.5	22.10	46.29	97	14.28	14.37	1.000	22.26	2.00	31.31	9.21	2.74
112	10-1-12	HB-5-DOPT-97-2	2	Das	HB	5	7.8	DOPT	22.5	22.10	46.45	97	14.28	14.42	1.000	22.26	2.00	34.42	12.32	3.43
113	10-1-12	HB-5-WOPT-97-3	3	Das	HB	5	7.8	WOPT	28.5	28.10	48.02	97	14.28	14.21	1.000	21.62	2.00	29.14	1.04	0.71
114	10-4-12	HB-5-OPT-94-1	1	Das	HB	5	6.9	OPT	25.5	25.10	45.91	94	13.84	13.91	1.000	22.26	2.00	29.36	4.26	1.37
115	10-4-12	HB-5-OPT-97-2	2	Das	HB	5	6.9	OPT	25.5	25.10	47.49	97	14.28	14.39	1.000	22.26	2.00	29.21	4.11	1.18
116	10-4-12	HB-5-OPT-100-3	3	Das	HB	5	6.9	OPT	25.5	25.10	48.48	100	14.72	14.66	1.002	21.62	2.00	27.95	2.85	0.58
117	10-8-12	BT-5-OPT-100-1	1	Chris	BT	5	7.4	OPT	23.3	23.30	49.87	100	15.35	15.24	1.01	22.32	2.00	30.37	7.07	6.34
118	10-8-12	BT-5-OPT-100-2	2	Chris	BT	5	7.4	OPT	23.3	23.30	50.00	100	15.35	15.36	1.00	22.26	2.00	30.07	6.77	6.41
119	10-8-12	BT-5-OPT-97-3	3	Chris	BT	5	7.4	OPT	23.3	23.30	48.59	97	14.89	14.96	1.00	21.65	2.00	29.85	6.55	4.69
120	10-8-12	BT-5-OPT-94-4	4	Chris	BT	5	7.4	OPT	23.3	23.30	46.92	94	14.42	14.20	1.02	21.69	2.00	30.67	7.37	4.80
121	10-10-12	HB-5-OPT-97-1	1	Chris	HB	5	7.5	OPT	25.5	33.09	47.41	97	14.29	13.54	0.997	22.31	2	38.21	5.11	1.20
122	10-10-12	HB-5-OPT-94-2	2	Chris	HB	5	7.5	OPT	25.5	33.09	45.91	94	13.85	13.12	0.997	22.25	2	36.43	3.34	1.20
123	10-17-12	HB-5-OPT-94-1	1	Chris	HB	5	7.27	OPT	25.5	24.73	45.91	94	13.84	13.96	1.000	22.32	2.00	33.88	9.15	3.5

124	10-17-12	HB-5-OPT-97-2	2	Chris	HB	5	7.3	OPT	25.5	25.62	47.27	97	14.29	14.24	1.002	22.26	2	32.49	6.87	5.00
125	10-17-12	HB-5-OPT-97-3	3	Chris	HB	5	7.27	OPT	25.5	24.73	47.34	97	14.29	14.46	0.995	21.60	2.00	33.78	9.05	4
126	10-17-12	EF-5-DOPT-97-4	4	Chris	EF	5	7.27	DOPT	21	24.03	39.17	97	14.80	11.93	1.003	21.71	2.00	54.54	30.51	27
127	10-21-12	HB-5-OPT-97-1	1	Chris	HB	5	7.48	OPT	25.5	25.58	47.44	97	14.29	14.36	0.997	22.31	2.00	32.81	7.23	5.4
128	10-21-12	EF-5-OPT-97-2	2	Chris	EF	5	7.48	OPT	24	25.58	48.37	97	14.80	14.56	1.003	22.25	2.00	50.01	24.43	24
129	10-23-12	HB-5-OPT-100-1	1	Chris	HB	5	7.7	OPT	25.5	21.98	48.78	100	14.72	15.08	1.005	22.32	2.00	32.30	10.33	6.14
130	10-23-12	HB-5-OPT-97-2	2	Chris	HB	5	7.7	OPT	25.5	21.98	47.41	97	14.29	14.71	1.001	22.26	2.00	32.72	10.74	4.70
131	10-23-12	EF-5-WOPT-97-3	3	Chris	EF	5	7.7	WOPT	27	27.81	49.41	97	14.80	14.76	0.993	21.60	2.00	48.80	20.99	20.90
132	10-23-12	BT-5-OPT-94-4	4	Chris	BT	5	7.7	OPT	23.3	24.09	47.21	94	14.42	14.42	1.000	21.71	2.00	30.31	6.22	3.10
133	10-25-12	EF-5-WOPT-97-1	1	Chris	EF	5	7.4	WOPT	27	23.48	49.58	97	14.80	15.24	0.998	22.30	2.00	51.89	28.41	24.70
134	10-25-12	HB-5-OPT-97-2	2	Chris	HB	5	7.4	OPT	25.5	24.12	47.38	97	14.29	14.14	1.023	22.27	2.00	31.19	7.07	2.60
135	10-25-12	HB-5-DOPT-97-3	3	Chris	HB	5	7.4	DOPT	22.5	24.12	46.16	97	14.28	14.18	0.994	21.60	2.00	34.23	10.11	2.91
136	10-25-12	HB-5-DOPT-97-4	4	Chris	HB	5	7.4	DOPT	22.5	24.12	46.07	97	14.28	14.13	0.996	21.71	2.00	33.12	9.00	3.00
137	10-30-12	HB-5-OPT-97-1	1	Chris	HB	5	7.2	OPT	25.5	26.77	47.27	97	14.29	14.08	1.004	22.32	2.00	29.29	2.52	2.35
138	10-30-12	HB-5-OPT-97-2	2	Chris	HB	5	7.2	OPT	25.5	26.77	47.30	97	14.29	14.12	1.001	22.25	2.00	48.42	21.65	1.81
139	10-30-12	HB-5-OPT-97-3	3	Chris	HB	5	7.2	OPT	25.5	26.77	47.26	97	14.29	14.16	0.998	21.58	2.00	44.41	17.64	4.40
140	10-30-12	EF-5-OPT-97-4	4	Chris	EF	5	7.2	OPT	24	24.62	48.46	97	14.80	14.67	1.005	21.70	2.00	52.53	27.91	27.75
141	11-2-12	HB-5-OPT-97-1	1	Chris	HB	5	7.2	OPT	25.5	27.41	47.40	97	14.29	14.04	1.004	22.32	2.00	35.83	8.42	2.78
142	11-2-12	HB-5-OPT-97-2	2	Chris	HB	5	7.2	OPT	25.5	27.41	47.30	97	14.29	13.95	1.009	22.26	2.00	34.65	7.24	2.49
143	11-29-12	EF-25-DOPT-97-1	1	Chris	EF	25	25.8	DOPT	22	22.16	47.65	97	14.80	15.01	0.995	22.31	2.00	43.82	21.65	17.04
144	11-29-12	EF-25-DOPT-97-2	2	Chris	EF	25	25.8	DOPT	23	22.37	48.00	97	14.80	15.11	1.000	22.25	2.00	42.47	20.10	16.81
145	11-29-12	EF-25-DOPT-80-3	3	Chris	EF	25	25.8	DOPT	22	22.16	39.32	80	12.20	12.27	1.008	21.60	2.00	47.22	25.05	8.70
146	11-29-12	EF-25-DOPT-80-4	4	Chris	EF	25	25.8	DOPT	23	22.37	39.71	80	12.20	12.37	1.008	21.71	2.00	43.04	20.68	6.68
147	12-1-12	EF-25-DOPT-97-1	1	Chris	EF	25	25.9	DOPT	21	20.85	47.37	97	14.80	14.98	1.000	22.34	2.00	41.10	20.25	12.60
148	12-1-12	EF-25-DOPT-97-2	2	Chris	EF	25	25.9	DOPT	21	20.85	47.39	97	14.80	15.00	0.997	22.27	2.00	41.49	20.64	14.26
149	12-5-12	TT-5-DOPT-85-1	1	Das	TT	5	6.8	DOPT	21.6	-	-	85	-	-	-	-	2	-	-	16.70
150	12-5-12	TT-5-DOPT-85-2	2	Das	TT	5	6.8	DOPT	21.6	-	-	85	-	-	-	-	2	-	-	15.40
151	12-5-12	TT-5-WOPT-88-3	3	Das	TT	5	6.8	WOPT	26	-	-	88	-	-	-	-	2	-	-	7.70
152	12-5-12	TT-5-WOPT-88-4	4	Das	TT	5	6.8	WOPT	26	-	-	88	-	-	-	-	2	-	-	6.90
153	12-9-12	TT-5-WOPT-88-1	1	Das	TT	5	7.1	WOPT	26	-	-	88	-	-	-	-	2	-	-	5.40
154	12-9-12	TT-5-WOPT-88-2	2	Das	TT	5	7.1	WOPT	26	-	-	88	-	-	-	-	2	-	-	8.40
155	12-9-12	TT-5-WOPT-88-3	3	Das	TT	5	7.1	WOPT	23.4	-	-	88	-	-	-	-	2	-	-	11.60
156	12-9-12	TT-5-WOPT-83-4	4	Das	TT	5	7.1	WOPT	23.4	-	-	83	-	-	-	-	2	-	-	10.40
157	12-11-12	EF-25-DOPT-97-1	1	Chris	EF	25	26.0	DOPT	18	18.22	46.12	97	14.80	14.86	1.005	22.33	2.00	45.39	27.17	19.38
158	12-11-12	EF-25-DOPT-97-2	2	Chris	EF	25	26.0	DOPT	18	18.22	46.18	97	14.80	14.88	1.005	22.26	2.00	45.90	27.67	19.37
159	12-11-12	EF-25-DOPT-97-3	3	Chris	EF	25	26.0	DOPT	14.5	14.29	44.63	97	14.80	15.06	0.995	21.83	2.00	46.23	31.95	19.72
160	12-11-12	EF-25-DOPT-97-4	4	Chris	EF	25	26.0	DOPT	14.5	14.29	44.79	97	14.80	14.79	1.013	21.49	2.00	46.68	32.40	21.36
161	12-17-12	EF-25-DOPT-97-1	1	Chris	EF	25	25.9	DOPT	18	17.90	46.14	97	14.80	14.99	1.003	22.32	2.00	46.01	28.12	21.13
162	12-17-12	EF-25-DOPT-97-2	2	Chris	EF	25	25.9	DOPT	18	17.90	46.22	97	14.80	15.09	1.000	22.25	2.00	45.19	27.30	22.39
163	12-17-12	EF-25-DOPT-97-3	3	Chris	EF	25	25.9	DOPT	14.5	15.00	44.73	97	14.80	14.82	1.005	21.83	2.00	46.09	31.09	23.57
164	12-17-12	EF-25-DOPT-97-4	4	Chris	EF	25	25.9	DOPT	14.5	15.00	44.72	97	14.80	14.88	1.210	21.48	2.00	46.77	31.77	22.34
165	2-3-13	TT-25-DOPT-97-1	1	Das	TT	25	25.9	DOPT	19.5	19.50	49.01	97	-	-	-	-	2.00	30.83	58.10	13.30
166	2-3-13	TT-25-DOPT-97-2	2	Das	TT	25	25.9	DOPT	19.5	19.50	49.00	97	-	-	-	-	2.00	32.14	64.82	12.00
167	2-3-13	TT-25-WOPT-97-3	3	Das	TT	25	25.9	WOPT	25.5	25.60	50.22	97	-	-	-	-	2.00	29.96	17.03	5.50
168	2-3-13	TT-25-WOPT-97-4	4	Das	TT	25	25.9	WOPT	25.5	25.60	50.47	97	-	-	-	-	2.00	30.66	19.77	5.90
169	2-6-13	TT-25-OPT-97-1	1	Das	TT	25	24.2	OPT	22.5	22.10	49.17	97	-	-	-	-	2.00	-	-	10.60
170	2-8-13	TT-5-OPT-97-1	1	Das	TT	5	8.2	OPT	22.5	22.10	49.17	97	-	-	-	-	2.00	36.43	64.84	15.10
171	2-8-13	TT-5-OPT-97-2	2	Das	TT	5	8.2	OPT	22.5	22.10	49.17	97	-	-	-	-	2.00	34.16	54.57	14.20
172	2-15-13	EF-25-OPT-94-3	3	Chris	EF	25	26.5	OPT	24	23.88	46.92	94	14.34	14.32	0.997	21.67	2.00	45.25	21.36	18.25
173	2-15-13	EF-25-OPT-94-4	4	Chris	EF	25	26.5	OPT	24	23.88	46.97	94	14.34	14.40	1.002	21.55	2.00	46.11	22.23	15.07
174	2-15-13	EF-25-OPT-97-1	1	Chris	EF	25	26.5	OPT	24	23.88	48.37	97	14.80	14.93	0.999	22.26	2.00	44.01	20.13	18.02
175	2-15-13	EF-25-OPT-97-2	2	Chris	EF	25	26.5	OPT	24	23.88	48.46	97	14.80	14.92	1.001	22.22	2.00	45.16	21.28	17.79
176	2-18-13	EF-5-OPT-94-2	2	Chris	EF	5	7.3	OPT	24	24.11	46.95	94	14.34	14.49	0.993	22.22	2.00	54.66	30.55	26.02
177	2-18-13	EF-5-OPT-94-3	3	Chris	EF	5	7.3	OPT	24	24.11	46.95	94	14.34	14.38	1.002	21.67	2.00	53.45	29.35	25.93
178	2-18-13	EF-5-OPT-94-4	4	Chris	EF	5	7.3	OPT	24	24.11	46.92	94	14.34	14.38	0.999	21.55	2.00	54.32	30.21	26.99
179	2-18-13	EF-5-OPT-97-1	1	Chris	EF	5	7.3	OPT	24	24.11	48.44	97	14.80	14.51	1.022	22.26	2.00	53.21	29.11	30.98
180	2-20-13	EF-5-OPT-94-1	1	Chris	EF	5	7.5	OPT	24	24.11	47.01	94	14.34	14.43	0.998	22.24	2.00	55.26	31.15	27.16
181	2-20-13	EF-5-OPT-94-2	2	Chris	EF	5	7.5	OPT	24	24.11	46.79	94	14.34	14.34	0.999	22.21	2.00	55.11	31.01	27.14
182	2-20-13	EF-5-OPT-94-3	3	Chris	EF	5	7.5	OPT	24	24.11	47.00	94	14.34	14.51	0.994	21.65	2.00	54.61	30.50	27.80
183	2-20-13	EF-5-OPT-94-4	4	Chris	EF	5	7.5	OPT	24	24.11	46.95	94	14.34	14.43	0.995	21.55	2.00	54.75	30.64	27.48

Appendix C: Training Material—PVR Method

TRAINING MATERIAL: PVR METHODOLOGY

The University of Texas at Austin

Available Methods

Three methods to calculate the Potential Vertical Rise (PVR) of an expansive soil are illustrated in this presentation:

1. Tex-124-E from TxDOT
   - Based on correlations of PI to swelling (traditional approach)
2. 6048 - Method A
   - Uses **a database** of swell test results on clays from the central Texas area, generated using centrifuge technology
3. 6048 - Method B
   - Uses **project-specific** swell test results on clays, generated using centrifuge technology

Example Problem

Problem Statement:

Consider a subgrade with a single stratum of Eagle Ford Clay

- Layer thickness = 10 ft
- ω = 27%
- γ = 121 pcf
- LL = 88%
- PI = 49%
- %< No.40 Sieve = 93%

Objective:

Calculate PVR using the three proposed methods. For Method 6048(A) use the available database of swell test results on Eagle Ford Clay. For Method 6048(B) use project-specific data from three centrifuge tests conducted using on-site.

Tex-124-E Methodology

- Modified Procedure from McDowell's 1959 method
  - Includes "Free Swell" conversion ratio
- Based on the correlation of PI to swelling potential
- Subdivide soil in layers
  - Typically uses 0.6 m (2 ft) sub-layers for simplicity

Tex-124-E Methodology

- From collected samples, determine ω, γ, LL, PL, PI, % Soil Binder (< No. 40 Sieve)
- Consider the following for the calculations:
  - Determine load on top and bottom of each sub-layer
  - Determine dry, wet, average moisture content
    - $\omega_d = .2 * LL + 9\%$
      - For EF, $\omega_d = 27\%$
    - $\omega_w = .47 * LL + 2\%$
      - For EF, $\omega_w = 43\%$
    - $\omega_a = 35\%$
  - Record moisture content, PI, % soil binder for each sub-layer

Tex-124-E Methodology

Information from the sub-layers considered in the calculation:

Depth (ft)	Thickness (ft)	Unit Weight (pcf)	Load at Top (psi)	Load at Bottom (psi)	Average Load (psi)	LL	Dry (%)	Wet (%)	w%	Dry/Avg /Wet	% Soil Binder	PI
0.0	2.0	121	0.0	1.7	0.8	88	27	43	27	Dry	93	49
2.0	2.0	121	1.7	3.4	2.5	88	27	43	27	Dry	93	49
4.0	2.0	121	3.4	5.0	4.2	88	27	43	27	Dry	93	49
6.0	2.0	121	5.0	6.7	5.9	88	27	43	27	Dry	93	49
8.0	2.0	121	6.7	8.4	7.6	88	27	43	27	Dry	93	49

Tex-124-E Methodology

- Determine percent volumetric change (1 psi surcharge) using PI from graph
  - % Vol Swell = 15%
- Determine swell under no loading

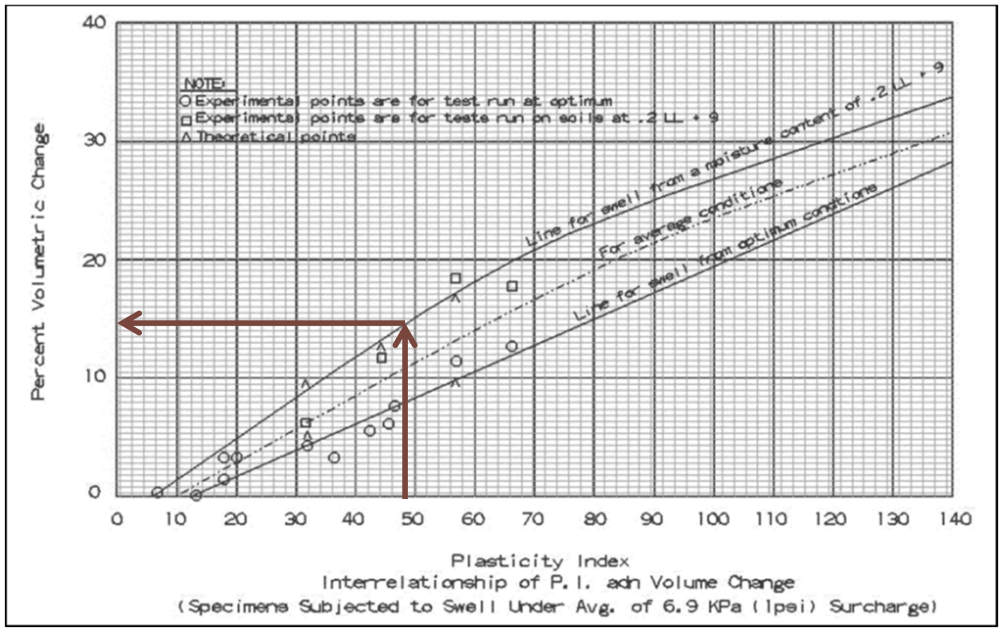

$$\%Free\ Swell = (\%\ Vol\ Swell\ @\ 1psi) * 1.07 + 2.6\%$$
$$= 15\% * 1.07 + 2.6\% = 18.7\%$$

Tex-124-E Methodology

- Determine PVR at top and bottom of each sub-layer using figures
  - Take load and go up to % Free Swell
  - From there, determine PVR in inches

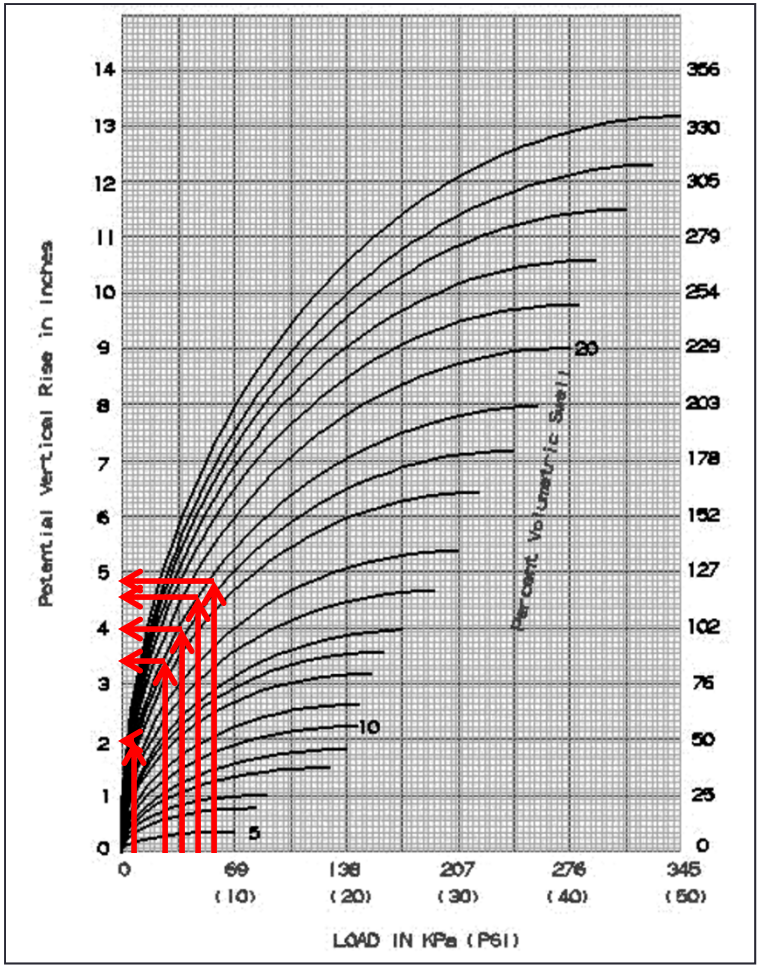

Tex-124-E Methodology

- Correction for Soil binder
  - Assumes that it is all passing No. 40
  - $C_{SB} = \frac{\%\ less\ than\ 25\ \mu m}{100\%} = \frac{93\%}{100\%} = .93$
- Correction for Wet Density
  - Assumes a density of 125 pcf
  - $C_{\gamma} = \frac{125\ pcf}{\gamma_a} = 1$
- Difference in PVR between top and bottom of sub-layer is the PVR of the sub-layer
- Multiply this by correction factors to get corrected PVR

Tex-124-E Methodology

Tex-124-E Calculations for each sub-layer:

Depth (ft)	Thickness (ft)	% Vol. Swell at 1psi	% Vol. Free Swell	PVR at Top (in)	PVR at Bottom (in)	Cor. Soil Binder	Cor. Density	PVR in Layer (in)	Cumulative PVR (in)
0.0	2.0	15	18.7	0	2	0.93	1.03	1.9	1.9
2.0	2.0	15	18.7	2	3.5	0.93	1.03	1.4	3.4
4.0	2.0	15	18.7	3.5	4	0.93	1.03	0.5	3.8
6.0	2.0	15	18.7	4	4.5	0.93	1.03	0.5	4.3
8.0	2.0	15	18.7	4.5	4.8	0.93	1.03	0.3	4.6

Calculated PVR using Tex-124-E Methodology: **4.6 inches**

Tex-124-E Methodology

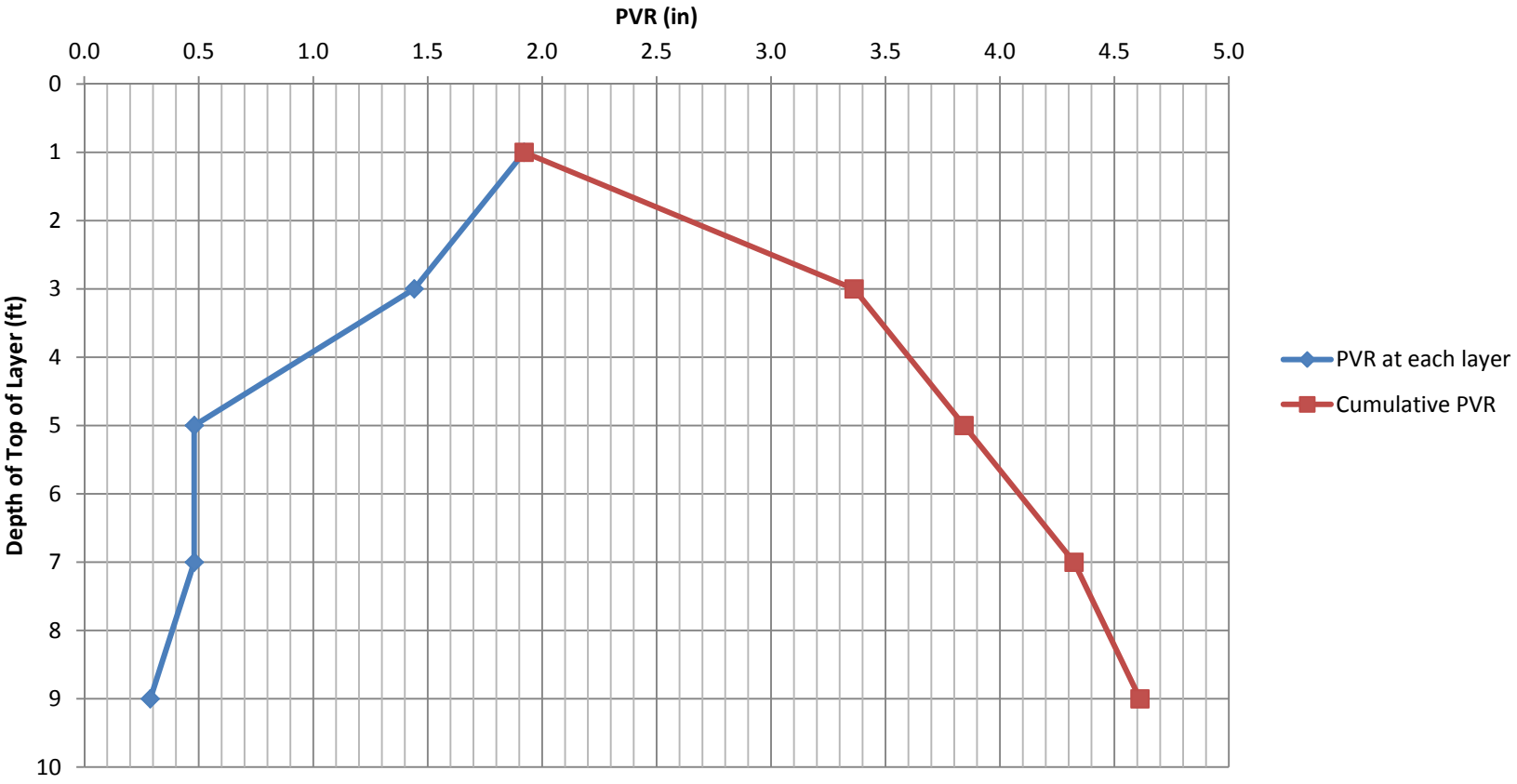

Proposed 6048(A) Methodology

- Proposed Methodology 6048(A) utilizes results from a database of centrifuge swell tests to predict the vertical rise soil.
- This methodology is useful for preliminary evaluations for locations where no centrifuge tests have been conducted using project-specific clay samples
  - Soil type of interest should be available in database
  - Current database includes soils from five locations from select sites around Austin:
    - Eagle Ford Clay
    - Black Taylor Clay
    - Tan Taylor Clay
    - Houston Black Clay
    - Soil 5 (generic fill)

Proposed 6048(A) Methodology

Procedure:

1. Information should be obtained (e.g. available boring logs) or inferred on water content, void ratio, and soil type with depth.
   - Can also get index properties, grain size distributions, etc.
   - *For this example, Eagle Ford clay will be used with a void ratio of 0.82 and unit weight of 121 pcf.*
2. Divide soil profile into sub-layers, two foot layers are typical.
3. Determine the effective stress at the top and bottom of each layer
4. From the matching curve in the database, obtain the average fully swollen void ratio (FSVR) for the range of stresses in each layer. The average FSVR may be taken:
   - as the FSVR corresponding to the effective stress at the center of the layer (less accurate)
   - as the FSVR corresponding to the log-average of the effective stress at the top and bottom of the layer
   - by calculating the average of the FSVR curve across the range of stresses in the layer (most accurate, requires integration)

Fully Swollen Void Ratio (Eagle Ford)

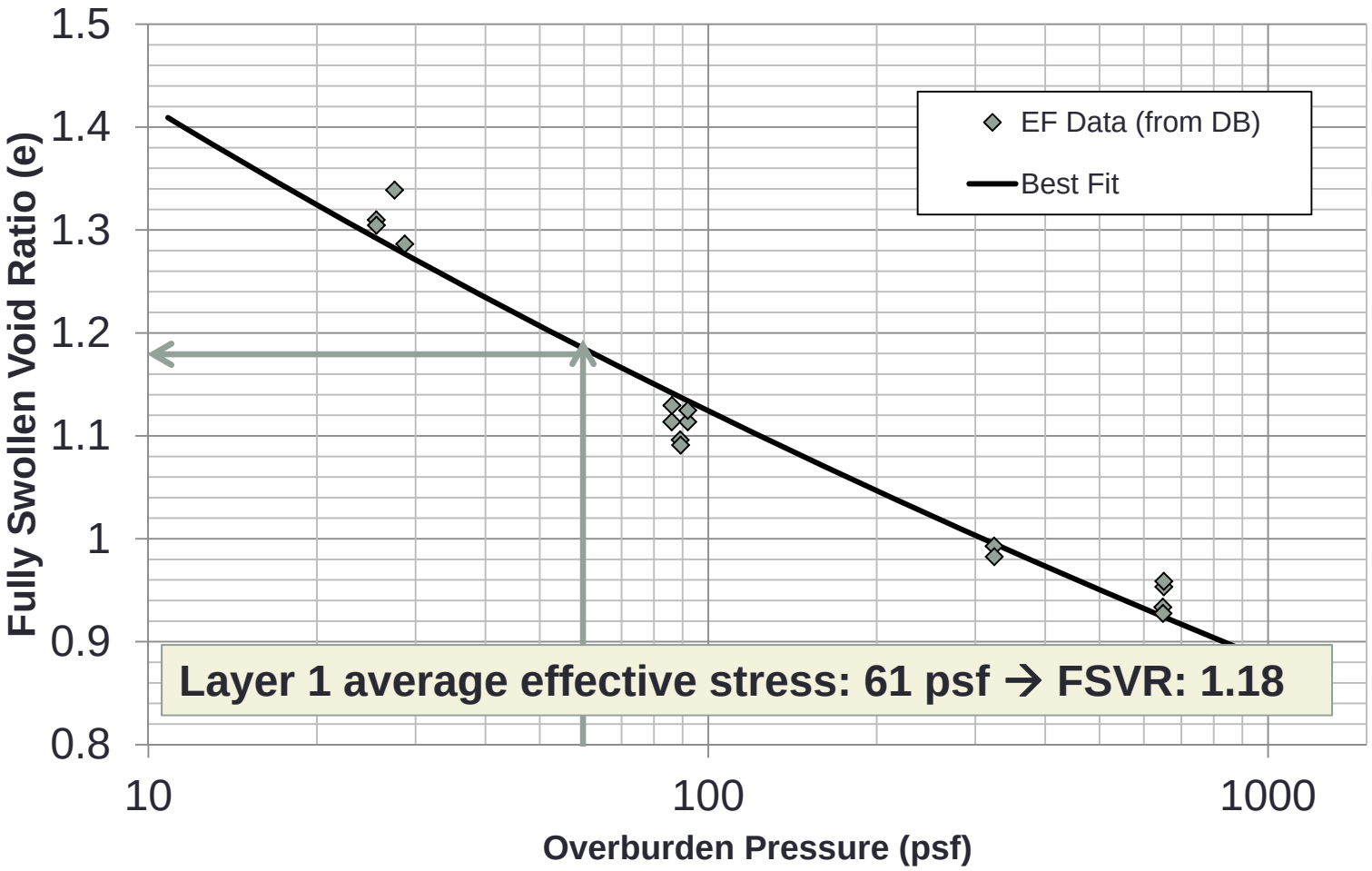

Proposed 6048(A) Methodology

5. Calculate the difference between the current void ratio and the predicted FSVR for each sub-layer
   - If the FSVR is less than the measured void ratio, the PVR of the layer is zero (this may occur for recently consolidated soils which were originally close to their FSVR, stress history of soil will also affect results)
6. Calculate the swell of each layer as a percent:

$$swell(\%) = 100\frac{\Delta e}{1+e}$$

7. Multiply swell by layer thickness to determine the PVR of a layer
8. Sum of PVR of each layer is the PVR of the soil

Proposed 6048(A) Methodology

6048(A) Calculations for each sub-layer:

Depth (ft)	Thickness (ft)	w%	Unit Weight (pcf)	Void Ratio (e)	Average Effective Stress (psf)	Fully Swollen Void Ratio (e)	Strain (%)	Vertical Rise (in)	Cumulative PVR (in)
0.0	1.0	27	121	0.82	61	1.18	0.20	2.44	2.4
1.0	1.0	27	121	0.82	182	1.06	0.13	1.60	4.0
2.0	1.0	27	121	0.82	303	1.00	0.10	1.24	5.3
3.0	1.0	27	121	0.82	424	0.97	0.08	1.01	6.3
4.0	1.0	27	121	0.82	545	0.94	0.07	0.84	7.1
5.0	1.0	27	121	0.82	666	0.92	0.06	0.71	7.8
6.0	1.0	27	121	0.82	787	0.91	0.05	0.60	8.4
7.0	1.0	27	121	0.82	908	0.89	0.04	0.51	8.9
8.0	1.0	27	121	0.82	1029	0.88	0.04	0.43	9.4
9.0	1.0	27	121	0.82	1150	0.87	0.03	0.36	9.7

Calculated PVR using proposed 6048(A) Methodology: **9.7 inches**

Proposed 6048(A) Methodology

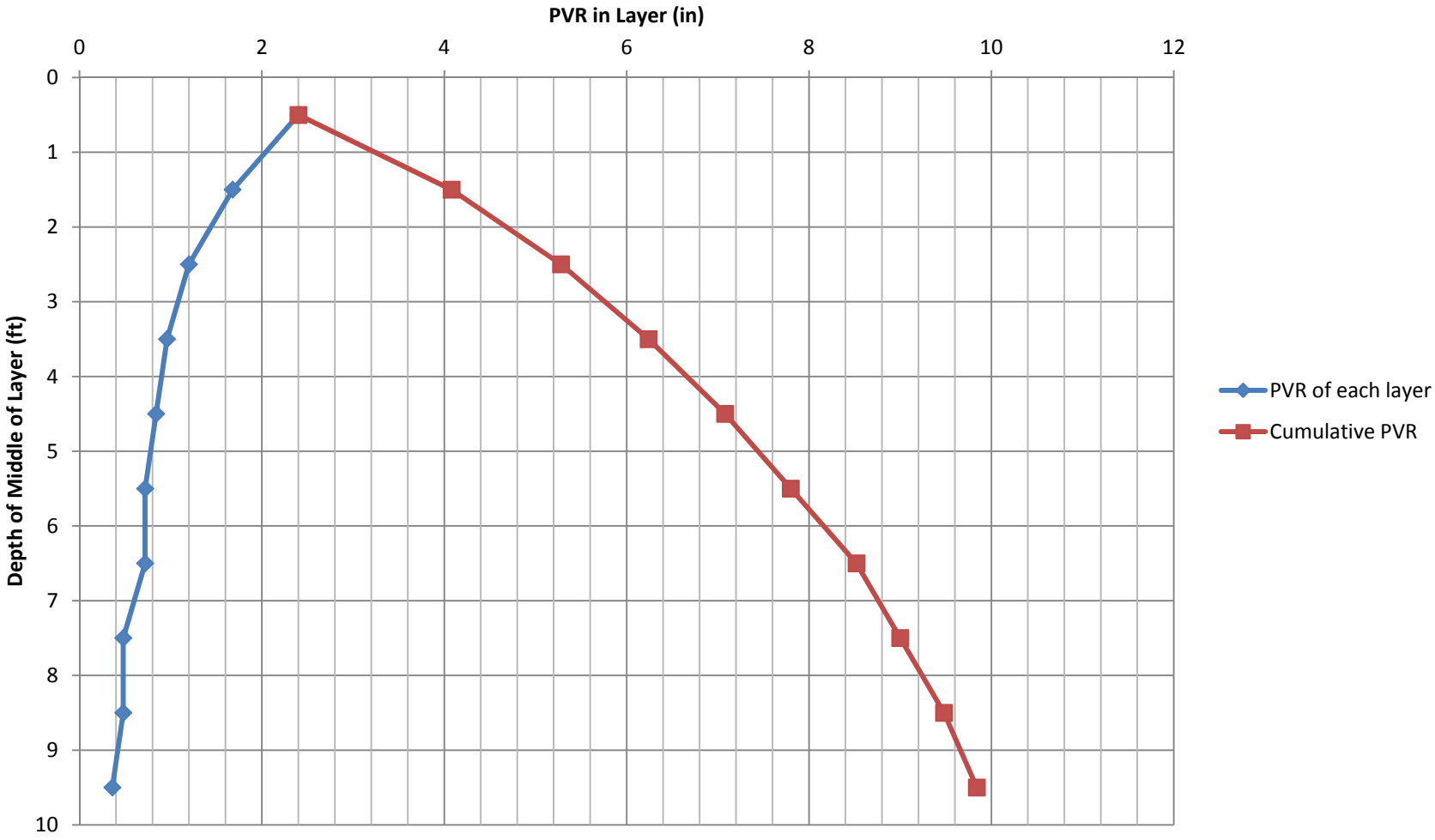

Proposed 6048(B) Methodology

- Based on directly testing in-situ sample in order to accurately predict the project-specific potential vertical rise
  - Undisturbed clay samples collected using Shelby tubes should be tested using the centrifuge at a variety of stresses (three g-levels recommended) in order to create a project-specific swell-stress curve
  - Determine the Swell-stress curve to predict swell of clay layer

Proposed 6048(B) Methodology

- Run centrifuge test at three different effective stresses (5g, 25g, 200g)
  - Determine effective stresses at top and bottom of sample
- Generate Swell vs. Effective Stress from centrifuge test results in order to calculate swell for each layer
- Multiply by height to determine PVR of each layer
- Sum of PVR for each layer is total PVR

Note on the Example used in this presentation: Undisturbed In-situ Eagle Ford samples were not available at this stage in the implementation project. Instead, a set of results from remolded clay samples were used for illustration purposes.

Proposed 6048(B) Methodology

- Determination of project-specific swell data using centrifuge samples tested at three g-levels:

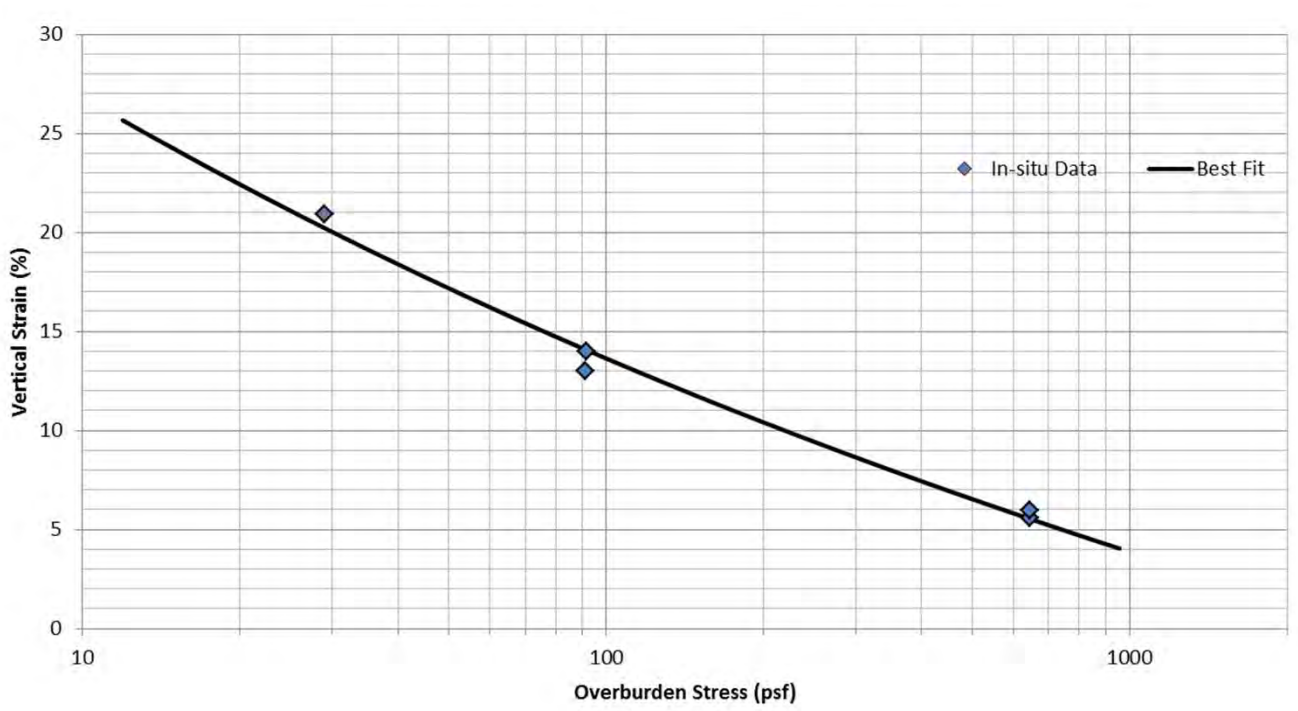

Proposed 6048(B) Methodology

6048(B) Calculations for each sub-layer:

Depth (ft)	Thickness (ft)	w%	Unit Weight (pcf)	Average Effective Stress (psf)	Swell (%)	PVR (in)	Cumulative PVR (in)
0.0	1.0	27	125	63	16	1.92	1.9
1.0	1.0	27	125	188	12	1.44	3.4
2.0	1.0	27	125	313	8.5	1.02	4.4
3.0	1.0	27	125	438	7.6	0.912	5.3
4.0	1.0	27	125	563	6	0.72	6.0
5.0	1.0	27	125	688	5.5	0.66	6.7
6.0	1.0	27	125	813	5	0.6	7.3
7.0	1.0	27	125	938	4	0.48	7.8
8.0	1.0	27	125	1063	4	0.48	8.2
9.0	1.0	27	125	1188	3.5	0.42	8.7

Calculated PVR using proposed 6048(A) Methodology: **8.7 inches**

Proposed 6048(B) Methodology

- Determination of swell for each sub-layer

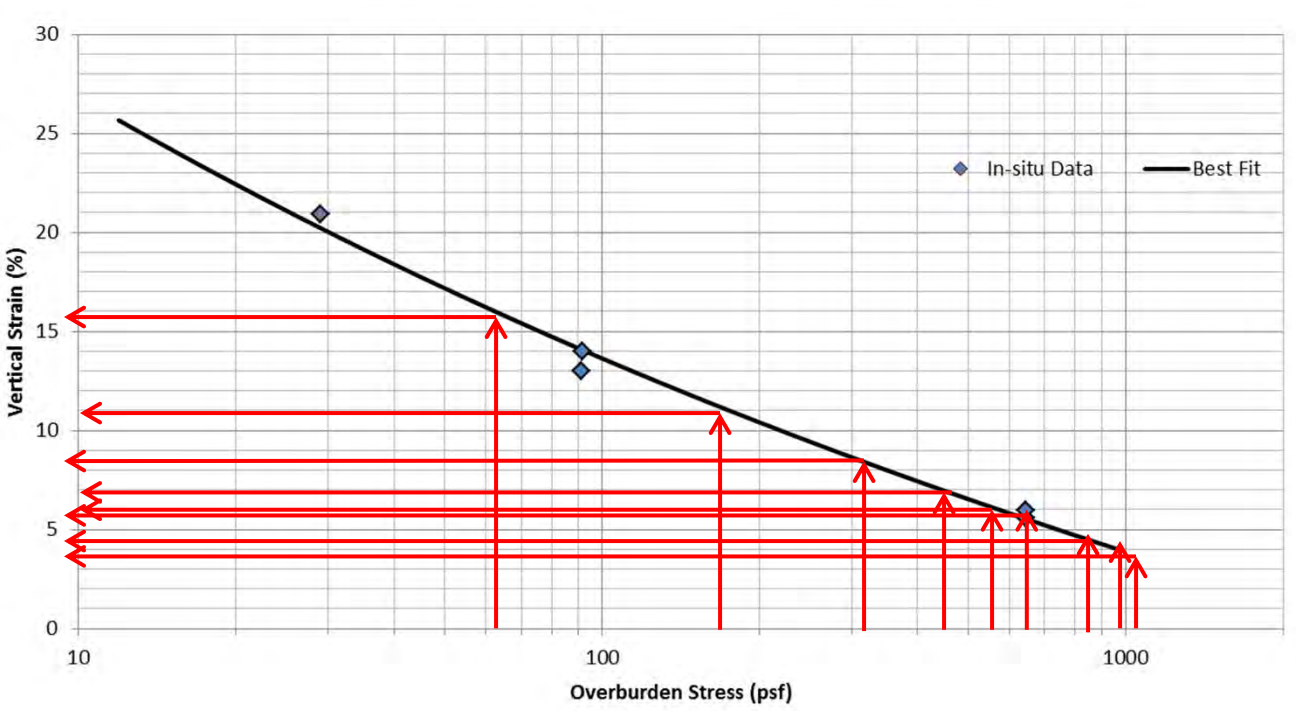

Proposed 6048(B) Methodology

Comparison of Cumulative PVR

Summary of PVR predictions using the various methodologies:

- Tex-124-E Methodology:
  - 4.6 Inches
- Proposed 6048(A) Methodology:
  - 9.7 inches
- Proposed 6048(B) Methodology:
  - 8.7 Inches

Comparison of Cumulative PVR

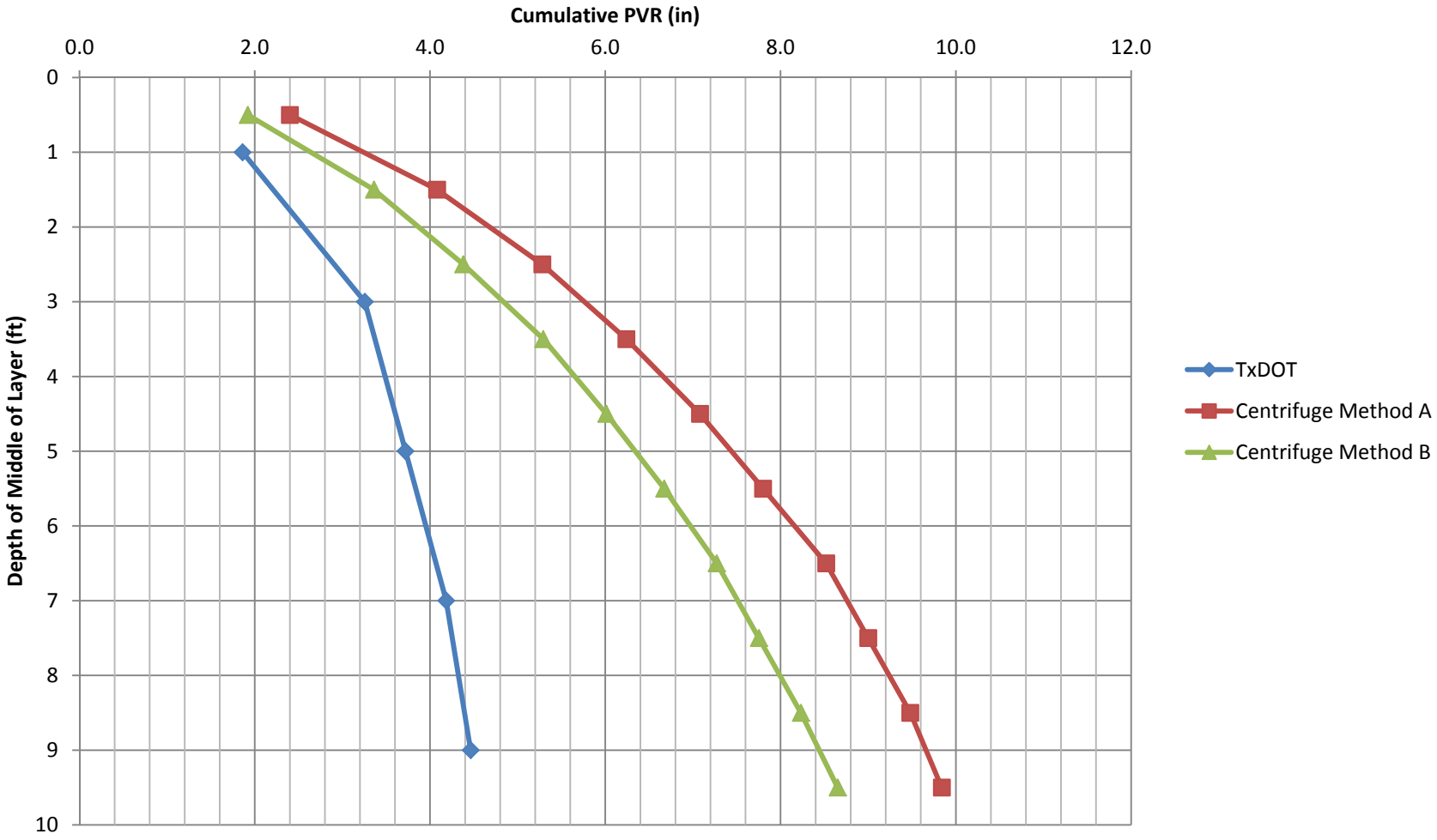

Final Remarks

- At least for the case of Eagle Ford Clay, the PVR calculated using Tex-124-E Methodology significantly underpredicts the vertical rise (by approximately 50%), when compared with the vertical rise obtained using soil-specific data
- The use of proposed Methodology 6048(A) is preferable to Tex-124-E as it leads to a soil-specific prediction of vertical rise.
- The use of proposed Methodology 6048(B) is recommended when project soil data is available. This approach leads to a project-specific prediction of vertical rise.
- At least for the example shown in this presentation, the PVR predicted using Methodologies 6048(A) and 6048(B) is similar (within approximately 10%). This is consistent with comparatively small variability in swell obtained in the database for results in the same clay but for different conditions/locations
- The use of a database (Methodology 6048(A)) is suitable for preliminary predictions of PVR.
- Methodology 6048(B) is recommended for prediction of PVR for final design
- Methodology 6048(B) cannot be implemented fully at this time, as the centrifuge equipment is not ready for testing undisturbed samples. Modification of the centrifuge cup sampler (to accommodate testing of undisturbed samples) is recommended.